Master's thesis

NTNU
Norwegian University of Science and Technology
Faculty of Engineering
Department of Mechanical and Industrial Engineering

Raoul Pathak

Resin Dosing for Closed Impregnation Filament Winding

Process Optimization

Master's thesis in Product Development & Materials
Supervisor: Kaspar Lasn
June 2019

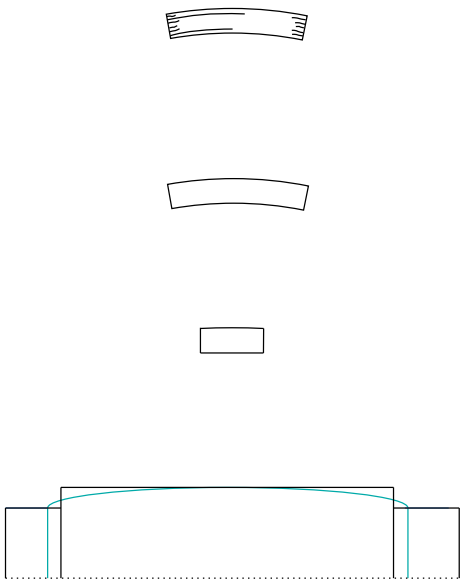

NTNU
Norwegian University of Science and Technology

HEXAGON

Raoul Pathak

Resin Dosing for Closed Impregnation Filament Winding

Process Optimization

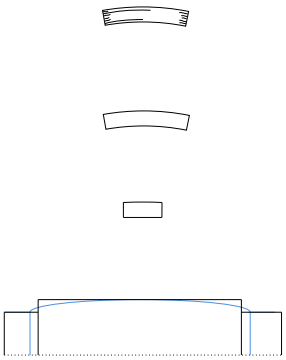

Master's thesis in Product Development & Materials
Supervisor: Kaspar Lasn
June 2019

Norwegian University of Science and Technology
Faculty of Engineering
Department of Mechanical and Industrial Engineering

NTNU
Norwegian University of
Science and Technology

Summary

This report covers an investigation into the use of using computer controlled administration of epoxy resin, or *resin dosing*, during filament winding, to optimize the short beam strength of carbon fibre reinforced polymer (CFRP) composites.

Use is made of a siphon based closed impregnation chamber, and a newly developed prototype for computer controlled resin dosing based on a peristaltic pump.

CFRP specimens have been wound in a hoop configuration across multiple resin dosing rates, and subsequent short beam strength testing has been done in accordance with standard ASTM D2344.

A curve showing the development of the short beam strength with increasing dosing rate has been produced. Some experimental work and analysis has also been performed with regard to variations in expired pot life.

Results indicate the presence of a transition zone featuring an increase in the short beam strength without an associated increase in thickness, as the composite becomes increasingly saturated.

Increasing the dosing rate beyond the point of visible saturation provides little gain.

The presence of such a point, the ability of the resin dosing system to change the dosing rate in a controlled way, and the ability for the short beam strength to reflect these changes are promising conditions for further parametric materials research and composite optimization efforts.

Changes in viscosity are shown to be significant long before the stated $4\,\mathrm{h}$ pot life is reached, and together with the observed effect of environmental conditions on pot life, these still pose a challenge to the control and repeatability of winding using electronic resin dosing for winding sessions exceeding $1\,\mathrm{h}$.

In depth considerations regarding the use of electronic resin dosing for parametric studies of mechanical properties are discussed, with emphasis on issues pertaining to peristaltic pumps, resin viscosity and pot life.

Preface

This study makes up my Master's thesis in mechanical engineering at NTNU. I was originally drawn towards this thesis last summer out of my interest for product development. Last semester I enjoyed creating the prototype resin dosing hardware. This thesis completes that arc, with a consideration of what such a tool can enable.

My thanks go to Håvard Hofstad together with Hexagon Composites for their support of this thesis, and for offering me my first summer job in engineering. I would also like to thank Kaspar Lasn for his guidance and in particular, his generous support, commitment and positivity towards the end of this thesis.

Many thanks must go to Per Anton for his advice and encouragement, to Johannes and Heidi for commiserating, and to Tore, Fridtjof and Petter for an enjoyable evening of puzzling together all my specimens after I had tripped and lost all 200 of them. And to Hans Theodor for introducing me to this lot. Ω

Raoul Pathak

Figure 1: Fixing a blunder

Table of Contents

List of Tables

List of Figures

Glossary

ADC analog-to-digital converter. 47

ASTM American Society for Testing and Materials, a standards organization.

CFRP carbon fibre reinforced polymer. 1, 19

COPV composite overwrap pressure vessel.

CSV comma separated values.

doctor blade Mechanical scraper or blade used in conjunction with a drum- or bath-type impregnation system to keep the tow from being too wet. 1, 6

duty cycle The fraction of a signal's period in which the signal is "active" or "high". Normally on a range of $0\,\%$ to $100\,\%$, but considered on a range of 0 - 255 for the purpose of this study. 13

FEA finite element analysis.

ILSS interlaminar shear strength. 15, 30, 35, 37, 40

IVW Institut für Verbundwerkstoffe - The Institute for Composite Materials, a German research institution. 6

neat resin Resin in its pure form, without reinforcement or other additions. 2

NTNU Norwegian University of Science and Technology. ii, vii, 1, 2, 4–9

PCA principal component analysis. 43

PLC programmable logic controller.

PTFE polytetrafluorethylene, also known by the trade name Teflon. 7, 47

PWM pulse width modulation. 13, 47

SBS short beam shear. 2, 24, 41

sizing filament coating which improves the compatibility between the fibre and matrix phases..

tex tex value, measured as fibre weight per length.

tow A single bundle of fibres, also known as a roving. 3, 4, 7–10, 17, 39, 47

Chapter 1

Introduction

1.1 Problem statement

A siphon based closed impregnation system for filament winding of carbon fibre reinforced polymer (CFRP) and an electronic, computer controlled resin dosing system have previously been developed at the NTNU composite lab[1] [4]. The objective for this thesis is to use electronic dosing to investigate if impregnation level can be optimized experimentally, with regard to resin use and short beam strength.

A theoretical consideration of the factors influencing the required impregnation is also to be made.

Resin dosing for filament winding is traditionally done at NTNU by a manually set doctor blade and is dependent on operator experience. Even then resin is wasted through dripping and repeated manual scraping of excess resin between layers.

In comparison to this traditional system, the aim is to reduce the amount of wasted resin while approximately maintaining the short beam strength of the composites impregnated traditionally. This is based on the assumption that the interlaminar shear strength only increases with the amount of resin present up to a certain point.

1.2 Motivation

The precision and repeatability offered by computer controlled administration of resin (”resin dosing”) affords a way to perform more accurate parametric studies of the relationship between process parameters and mechanical properties of the finished composite. This can open the way for further understanding composite behavior, and for optimization of production processes.

[1] At the NTNU Department of Mechanical and Industrial Engineering

The experimental part of this study has emphasis on the relationship between the resin dosing rate and the short beam shear (SBS).

It is hypothesized that as the impregnation level increases from an extreme low end to an extreme high one, the interlaminar shear strength will only increase proportionally with the impregnation level up to a certain point, until the composite is saturated and excess resin either drips off during winding or lays on top of the composite as neat resin. When increasing the resin dosing rate above this point, strength should either increase much more slowly, or remain the same.

Currently, filament wound composites at the NTNU composites lab are impregnated by a drum impregnation system which is set to introduce too much into the composite, followed by the operator manually scraping off excess resin between each layer.

The intended outcome of this study is not a specific dosing rate to be recommended for use, as this is relative to the specific fibre and resin used and is further dependent on a multitude of factors in the winding setup and composite being produced. Rather, it will present considerations regarding parametric studies as a method of establishing an optimum dosing/impregnation rate.

Further motivation for the experimental work in this study is to validate the development of the machine developed in a previous study [5]. Answering whether it is indeed able to impregnate composite rings to various degrees, whether this is a repeatable process and whether the resin quantity deposited on the mandrel is approximately as one would expect.

1.3 Scope

The aim of this study is not to optimize mechanical properties as a whole. In practice, there are several mechanical properties such as tensile strength, fatigue life, impact resistance, and stiffness, which will not be considered as part of this study. Furthermore, the stresses incurred by the short beam shear are complicated and one cannot directly relate the strength to a specific mechanical property[6]. However, the test is predominantly one of matrix properties. Helical winding patterns and complete pressure vessels are outside of the scope of this study, only hoop wound specimens shall be considered.

Chapter 2

Background and theory

2.1 Filament winding

The nature of composites as highly application-tailored materials has led to the development of specialized manufacturing methods. Filament winding is one such method, used to produce continuous-fibre reinforced composite products such as pressure vessels, driveshafts, rocket hulls, and other products featuring convex geometry, and usually rotational symmetry. An example of a filament wound pressure vessel is shown in figure 2.1

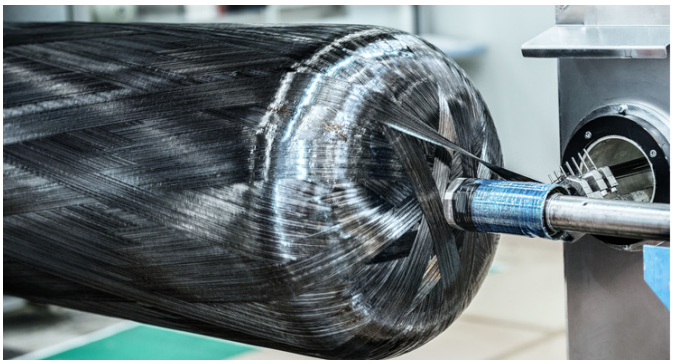

Figure 2.1: Carbon and glass fibre CNG vessel, manufactured by Hexagon Raufoss[1]

During filament winding, one or multiple fibre tows (commonly glass or carbon) are held on spools, in either a dry state or pre-impregnated with resin. During winding they are led around the mandrel, which defines the basic shape, by a winding eye which moves along the mandrel, guiding the tows to create certain patterns.

2.2 Fibre impregnation

If dry fibres are used, they will go through a resin impregnation system between the spool and the winding eye. Here resin is applied to the tow and the tow is manipulated by rollers or scrapers, in order for the resin to be absorbed as well as possible.

Impregnation systems commonly make use of a resin bath, a simple tray filled with resin. Such systems are known as open impregnation systems. In one variant of open impregnation, shown in figure 2.2, the tow is led by a series of rollers along a path through the bath.Resin is applied to the tow as it is completely submerged, and the subsequent rollers aid in impregnation by having the tow compress and spread out against the rolling surface. The exposed surface area increases, air escapes the tow more easily and surface tension pulls resin into the tow interior. Further rollers and/or scrapers act to remove any excess resin, which pours back into the tray.

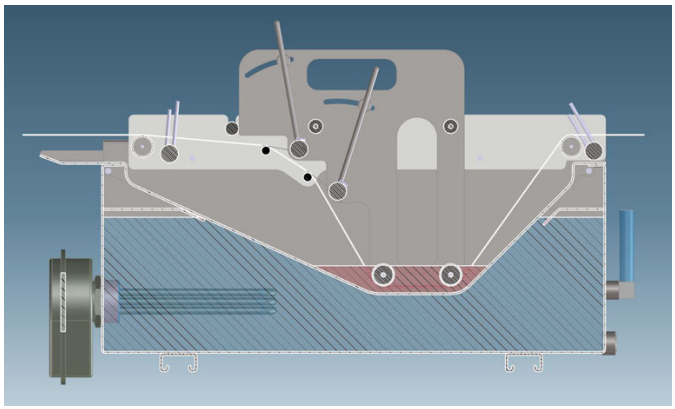

Figure 2.2: Open impregnation schematic, showing the resin bath and rollers [2]

In another variant, shown in figure 2.3, the tow is passed tightly over a drum which is partially submerged in the bath. As the drum rotates, a layer of resin adheres to the drum, and the tow is submerged only in this layer of resin that is carried along. The tow is spread out sufficiently in contact with the drum such that no other rollers are needed after except for the one constraining it against the drum. The standard impregnation system used at NTNU uses this principle.

With so-called closed impregnation, tows are led through a cavity into which resin is injected. One design for a closed system makes use of an S-shaped tube (referred to as a ”siphon” in the original work) and no moving parts to impregnate the tow. A prototype for such a system has been developed at NTNU. It is based on the closed impregnation system developed at the Institut für Verbundwerkstoffe in Germany[7].

The tow is led through an S-shaped siphon filled with resin. As the tow is pulled through it is forced into contact with the siphon in 3 zones, where the resin impregnates the tow.

The more controlled circumstances provided by a closed impregnation environment provide a useful starting point for computer controlled resin dosing.

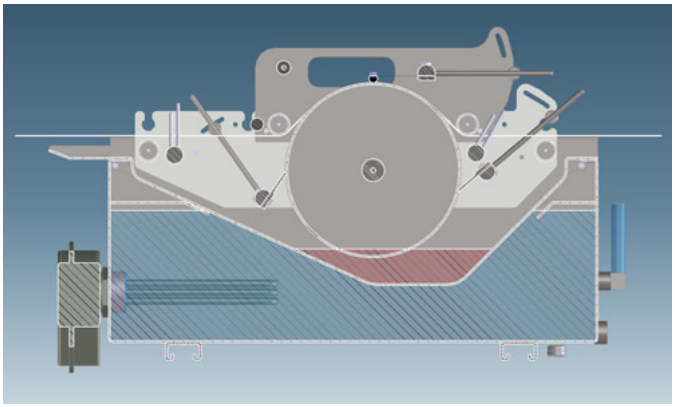

Figure 2.3: Drum impregnation schematic [3]

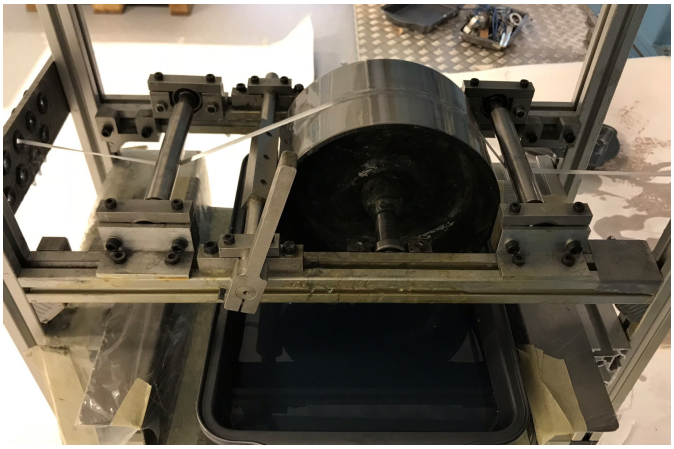

Figure 2.4: Drum type impregnation system currently in use at NTNU

2.3 Traditional impregnation system

The existing impregnation system present at the NTNU composite lab is a drum-type open impregnation system, shown in figure 2.4.

The scraper, or so called doctor blade consists of a simple metal block which is manually adjusted to sit at a certain distance from the drum. It requires operator experience to know the correct setting for winding. This tends to be "implicit knowledge" which is hard to document.

In the course of the preceding study, observations were made at two occasions where the filament winding machine was used in the autumn of 2018[5]. One dry-winding demonstration was given by an earlier user of the system and one composite was wet-wound. Process observations made at these two occasions, as well as questions asked to other users of the filament winding machine, motivated the development of a novel resin dosing system. The practical concerns can be summarized as follows:

- The winding process at the lab is very operator dependent. Appropriate settings for the doctor blade, and appropriate appearance of wetness are roughly estimated during winding and are often set by trial and error going on throughout a winding session. Answers to questions concerning the right settings for winding simple cylinders are mostly limited to "change until it looks right".
- To ensure good impregnation, winding is usually done too wet and excess resin is removed from the mandrel as the composite is wound, by scraping a hand over the surface at certain times, to a degree which is hard to quantify.
- The amount of resin required to impregnate a given composite is in practice not quantified, and impregnation might need to stop in order to mix more resin, or much resin might be left over after winding.

Taking research concerns into consideration, the system brings further challenges:

- The dosing rate is not directly quantifiable and therefore not directly transferable to other systems, which likely feature different parameters or technologies. This makes empirical relationships harder to analyze.
- Dosing is not easily repeatable from trial to trial under changing or even static conditions.

The traditional system is representative of the systems most commonly used in the industry[8]. However, systems which use electronically positioned scrapers do exist [9]. The closed impregnation system developed at IVW[1] features electronic resin injection.[7]

2.4 Introduction to the novel impregnation and dosing system

The system used during this study can be considered as two parts - the siphon based closed impregnation chamber, and the electronic resin dosing system that pumps resin into the

[1] Institut für Verbundwerkstoffe

siphon, both pictured in 2.5. The closed impregnation chamber is the results of a previous study at NTNU[4].

Figure 2.5: Figure showing the siphon based closed impregnation unit and the resin dosing system

The siphon shape and PTFE material were in that study found to sufficiently impregnate composites. This siphon was originally used with gravity fed resin administration which was constricted by a screw clamped onto the resin feeding tube. The screw was to be set once at a level deemed appropriate by trial and error, and left so for the duration of the winding session.

The electronic resin dosing system was developed as an improvement to this, and design and development of a prototype electronic dosing system was the subject for the study made by the author in the autumn of 2018[5], which resulted in the physical prototype used for this study.

An overview of this prototype resin dosing system hardware is given in figure 6.1 and 6.2 in the appendix.

2.5 Resin dosing dependencies

The resin dosing rate is influenced by a multitude of factors constituting the winding process. An overview of significant theoreticized factors is given below.

The dynamics of the impregnation process occurring within the siphon are not considered here. These are described in more detail in the original work[4]. Behavior has also been modeled on a microscopic level by Institut for Verbundwerkstoffe [10]. Emphasis in this study is on considerations at the macroscopic level.

The impregnation mechanism can be treated as a black box to a certain extent, where flow rate in equals the flow rate rate out, and the siphon acts as a stabilizing factor (where a fuller siphon leads to a wetter tow exiting the siphon/unit) creating steady state conditions,

within limits - As long as dosing is not so excessive that it spills from the siphon during winding.

While the concerns of electric motors, voltages and duty cycles (described further in section 3.2 are implementation details not immediately relevant to composite research, they represent the effect of differences in flow resistance (which will influence the movement of resin throughout the system no matter the pumping technology used) which is relevant no matter the pumping technology in use. Even purely mechanical gravity fed or a drum impregnation system is influenced by these factors.

Earlier use of the drum impregnation system at the NTNU composite lab has shown that the drum picks up more resin towards the end of a typical winding session than it does at the beginning.

A non-exhaustive overview of the significant factors can be found below and hints at the complex nature of the problem.

- **Sizing** Carbon fibres are subject to a surface treatment to increase the bonding with the matrix material. The various sizings used by different carbon fibre manufacturers have different resin uptake properties. [11]

- **Fibre tension** A higher fiber tension creates a more compact composite. A lower associated matrix volume fraction therefore requires a lower resin dosing rate. A parametric study of the influence of fibre tension on composite quality has been done by[12].

- **Fibre speed** The resin dosing rate should ideally be directly proportional to the winding speed, but the dependence of other factors on the winding speed complicate this relationship. The speed itself may also be a dependent factor, as in a filament winding system where the mandrel rotation speed is controlled rather than the filament payout speed, the filament speed will be dependent on the radius and even the thickness of the already wound composite.

- **Viscosity and curing behavior**

  - **Resin viscosity** The viscosity of the resin influences the uptake and distribution of resin into the tow, but also the pumping resistance met by the peristaltic pump as described by the Darcy-Weisbach equation[13], and therefore changes the flow rate for any given input voltage. Other pumping mechanisms such as the gravity fed dosing used previously by [4] or the traditional drum based impregnation system are to varying degrees subject to the same dependencies on viscosity, through the changing Darcy friction factor .
  - **Room temperature and humidity** The curing rate and pot life of the resin are strongly dependent on environmental conditions such as room temperature and humidity. Curing is accelerated and pot life decreased at higher temperatures.
  - **Resin bath temperature** Some resin baths may feature cooling to extend pot life. Even the shape in which the resin is held is an influence, as the resin is exothermic and the proportion of volume to surface area changes the heat dissipated during the course of the pot life and winding session.

- **Losses**
  - **Downstream surfaces** in practice, nearly all guiding surfaces downstream of the impregnation chamber or bath, such as the winding eye, spreader, or any wheels, will scrape or absorb part of the applied resin. This leads to a certain amount of loss of resin which poses an environmental and cost issue of waste by itself. In relation to resin dosing, the issue is whether the amount of loss is reliably quantifiable so that it may be compensated for.
  - **Overdosing, dripping** To achieve good quality impregnation at the NTNU composites lab, current practice is to excessively impregnate the tow with resin and to manually remove excess resin from the mandrel in between each wound layer by hand, and remove excess resin after winding has completed either by hand or the application of a peel ply[2]. Computer controlled resin dosing has the potential to reduce a large amount of resin waste by negate the need for most of these practices.
- **Winding pattern** Hoop layers are by their unidirectional nature a more compact arrangement of fibres than interwoven helical layers, and therefore require less resin. For a product such as a pressure vessel which will feature a combination of hoop and and helical layers, the ability to change the dosing rate on the fly during winding can ensure that the appropriate amount of resin is always being applied.
- **Position along mandrel** When winding a pressure vessel, the composite is subject to extra compaction in the areas around the domes, and ideally the dosing rate should be lower accordingly.

Characteristics such as viscosity and resin temperature are time dependent. Furthermore, most of these factors are clearly interdependent to various degrees. For instance, the dripping and losses of resin may depend on the viscosity. Another example is the fibre tension which in reality is the sum of the tension generated by the tension mechanism in the creel and the friction generated in the impregnation unit. As conditions such as viscosity change, so will the generated friction resulting fibre tension, as shown by the free body diagram in figure 2.6. Depending on the desired level of precision, the modelling of the winding process can become intractably complicated.

2.6 Other significant parameters

Apart from the dosing rate, other parameters are of significance to the winding and impregnation process:

- **Pulsation** A peristaltic pump by nature outputs a pulsed flow, and reducing the flow rate by reducing the motor speed of a peristaltic pump, will also lead to greater time between pulses. Depending on the impregnation method in use, this could mean that the tow is unevenly impregnated. The siphon based closed impregnation unit used in this study is assumed to have characteristics which greatly lessen the

[2]This is done to increase composite compaction and also to avoid the issue of amine blush[14]

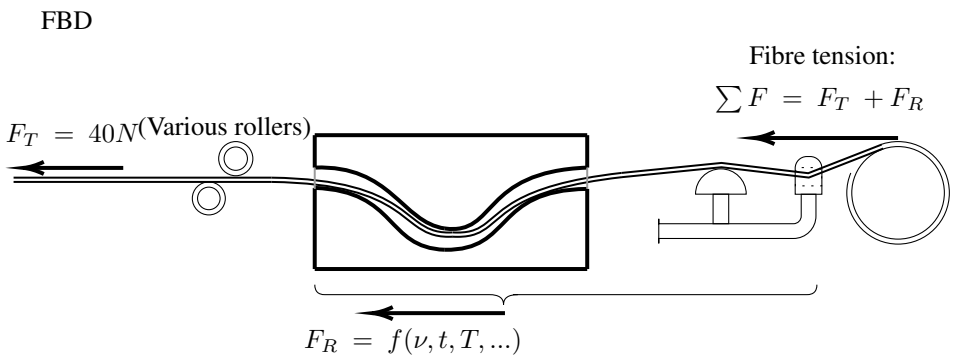

Figure 2.6: Free body diagram showing forces on impregnation unit and mandrel

impact of pulsations with a duration in the range of a few seconds or less, as the bottom of the siphon will act as a reservoir that dampens out pulsations in the flow entering the chamber, such that the tow leaving the chamber is more homogeneous. Commercially, peristaltic pump pulsation dampeners exist[15]. These operate on principles similar to the one taking place in the siphon, described above.

- **Transients** Although the reservoir of resin in the siphon will smooth out pulses from the peristaltic pump, it also causes a transient when changing from one dosing rate to another. The shape of this transient could be difficult to determine analytically based on the mechanisms at play in the impregnation chamber, and for some time the exact dosing rate could therefore be unknown, as shown in figure 2.7. This is not expected to be an issue for the fidelity of winding that is being done in this study, but for theoretical future filament winding techniques that make better use of computer controlled dosing, it could be imagined that composite winding processes are designed with more dramatic changes in dosing rate from one hoop or layer to the next. Transients then complicate the matter in a way which must be solved by either modelling the transient behavior, or physically reducing the volume of the puddle by a change in the design of the closed impregnation unit.

- **Time delay** There is a time delay for the fluid traveling the impregnation chamber via the fibre to the mandrel, which affects the responsiveness in changes to the dosing rate during winding. There is in theory no time delay from the bucket of resin via the pump to the impregnation chamber, as the whole silicone tube is filled with resin and any movement of fluid is instantly reflected across the entire tube.

  When winding with a pre-planned dosing configuration, time delays can be mitigated even for exotic dosing strategies with rapid changes, simply by pre-empting the time delay and make the change ahead of when it is needed on the mandrel, based on the fibre speed and distance between the mandrel and impregnation unit. However, with the potential of introducing closed-loop control to a resin dosing system, this issue becomes more pressing. Time delays are system non-linearities which complicate closed-loop control strategies significantly[16].

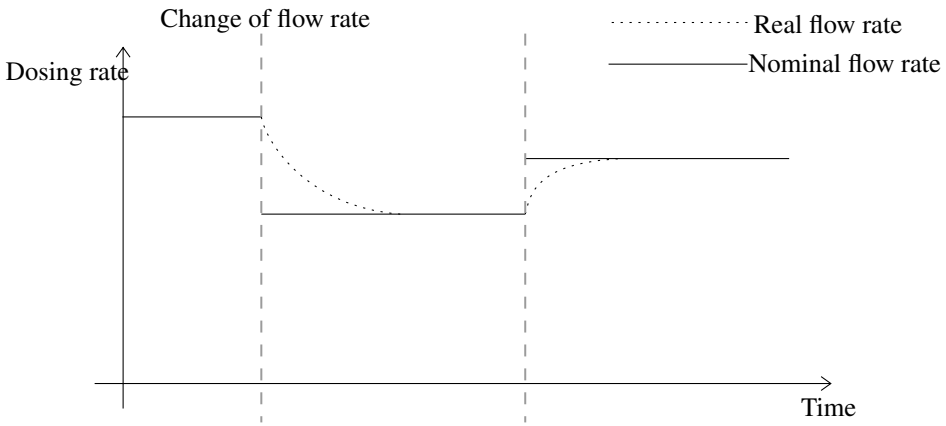

Figure 2.7: Impregnation level during a transient from one nominal rate to another

Chapter 3

Method and materials

As this study is a parametric study, it is necessary to generate a lot of experimental data under similar circumstances with only a single parameter being changed. There is therefore a strong requirement for systematic and precise treatment of the entire process: winding, cutting, measuring and testing.

3.1 Materials Used

The epoxy system and fibres used for this study are specified in figure 3.1.

Equipment/material	details
Winding machine	Mikrosam
Carbon fibres	Mitsubishi Rayon/Grafil 34-700 WD
Filament count	12000
Epoxy system	Hexion Epikure RIMR 135 + RIMH 137
Mandrel	140 mm diameter polyethylene pipe

Table 3.1: Equipment and materials used

3.2 Flow rate calibration

The pump rotation is set through a pulse width modulation (PWM) signal which has a variable *duty cycle*, [1] which on the motor side is perceived as voltage on a range of $0\,\mathrm{V}$ to $12\,\mathrm{V}$. Figure 3.1 shows why an analytical relationship between the instructed signal and the resulting flow rate is hard to obtain. For this reason, calibration of the pump flow rate was needed.

[1] normally on a range of $0\,\%$ to $100\,\%$, but considered on a range of 0 - 255 for the purpose of this study as that is what the microcontroller deals with

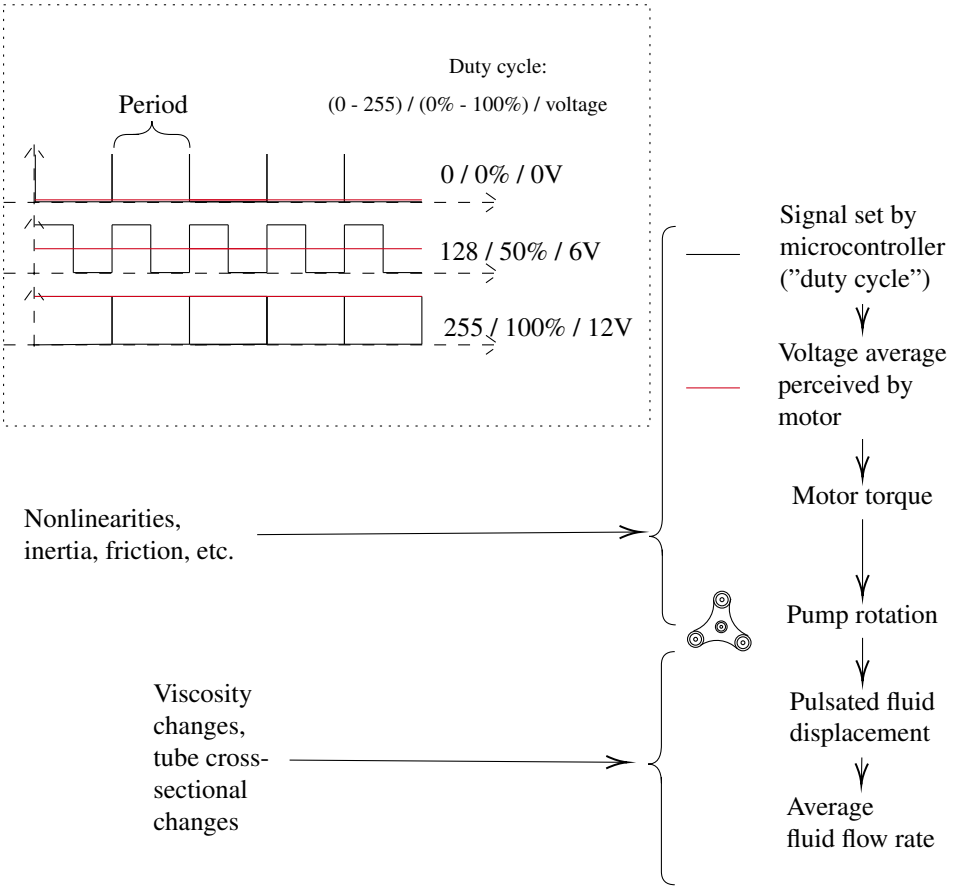

Figure 3.1: Steps between the duty cycle setting and the flow rate of the pump

As the directly controlled parameter for this study is the duty cycle, the voltage over the motor was not directly measured, and the calibration process has some uncertainty as described in section 5.4, reference in this report will for the purpose of accuracy be given to the duty cycle where possible.

Voltages were calibrated against flow rates, and the lowest achievable flow rates determined, by pumping resin for one minute at a time at various duty cycles and and weighing the pumped resin.

For this report, flow rates are always considered *mass* flow rates.

Dosing was found to be unreliable below a duty cycle of 130 due to a lack of torque.

In terms of flow rates (presented in section 4.2, this means that it couldn't even reach a third of its maximum flow rate. Meanwhile, a step down in tube size implies a 4x reduction in cross sectional area - so from a duty cycle of 130 and below, a kind of "intermittent pumping" was performed, by turning the pump on and off in timed intervals at a fixed voltage. The voltage is high enough to enable to motor to rotate, and with by changing the interval of pumping, the flow rate can be controlled and reduced further.

This was only needed for the lowest dosing rates of the 3.2 mm tube, to be able to "reach down" to the next available tube size. In this way the most interesting range of dosing rates (presented in section 4 could be explored.

This "intermittent pumping" should not be confused with the pulsed output ordinarily produced by a peristaltic pump, however this does direcly lead to an even more pulsated flow than the pump ordinarily exhibits.

3.3 Winding

To be able to produce a large number of specimens at many different dosing rates without having to produce an excessive number of cylinders, specimen winding was done in the form of multiple separate *rings* for each cylinder, each with its own dosing rate.

As the shoulders or edges of each ring slipped slightly from their nominal positions (The windings slip to become wider but thinner towards each edge), specimens were taken from the centre of each ring so that the through-thickness composition of the specimen was as close to nominal as possible.

As rings were initially wound without any spacing, the the abovementioned slipping also led to a different profile for the first two cylinders which were wound. This is detailed in figures 3.2 and 3.3.

Times were noted for when resin was mixed and when winding started, and the duration of winding for a ring at a given speed was noted.

The set fibre tension was $40\,\mathrm{N}$

3.3.1 Layup and winding configuration

All interlaminar shear strength (ILSS) specimens consist of 19 unidirectional[2] layers of fibres wound in a hoop configuration, at close to 90° to the mandrel. A 20 layer hoop wound composite has been commonly used at the department for ILSS testing, but an odd number

[2]

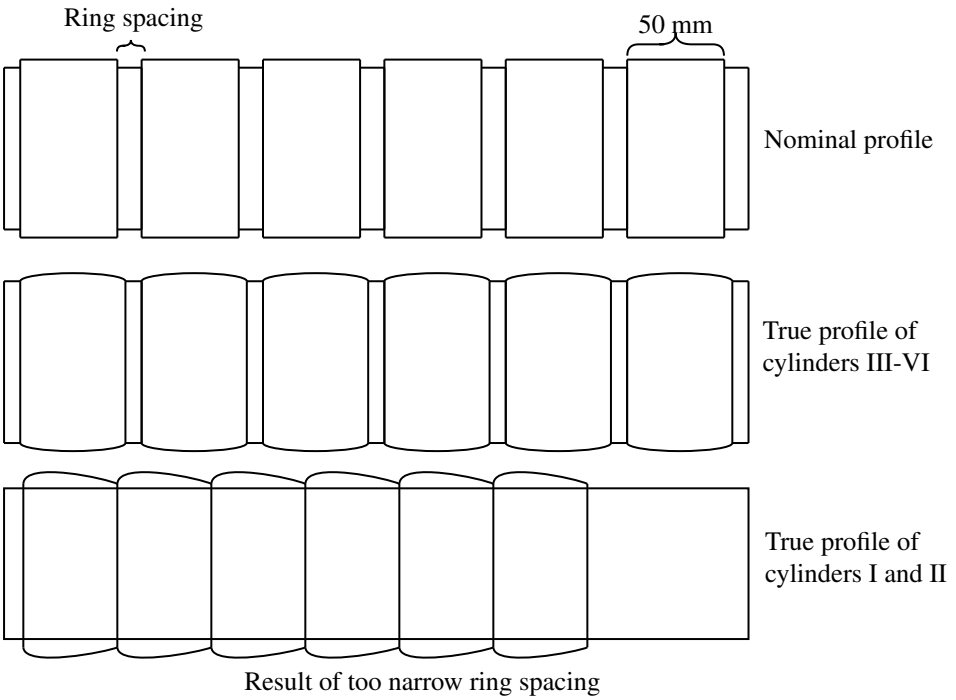

Figure 3.2: Change in profile caused by wound rings slipping at each end

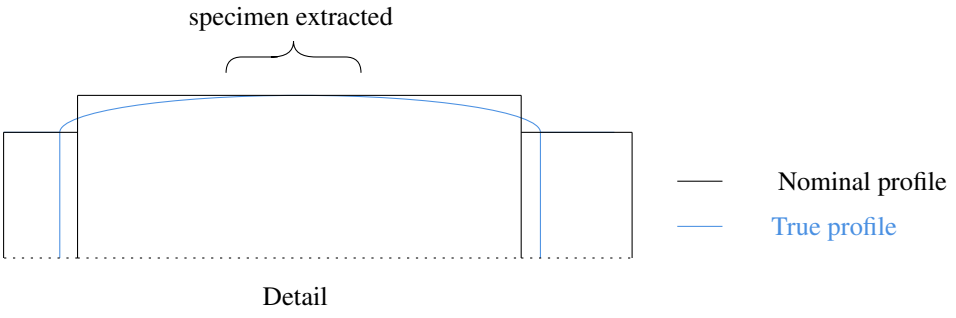

Figure 3.3: Detail on the change in profile

of layers was chosen because this allows continuous winding of rings with different levels of impregnation, without needing to stop the machine, cut the tow and reattach it for a new ring. This prevents any transients associated with starting or stopping the winding and impregnation process and allows process parameters to be as close to steady state as possible.

Pumping speeds were changed ”manually” via computer input by an operator, when the winding eye moved from one ring to another.

3.3.2 Winding speeds

Speeds on the filament winding machine are defined by a base speed and a percentage multiplier ranging from $1\,\%$ to $200\,\%$. The base speed is defined in the Mikrosam filament winding layup software ”Winding Expert”, and the speed multiplier is set in the filament winding operation software ”Winding Commander”.

The base speed setting used for all winding done for this study is $20\,\mathrm{m/s}$. The speed multipliers for the various cylinders can be found in table 3.2. $40\,\%$ was considered the baseline setting.

Cylinder nr.	Nr. of rings.	Base speed	Speed multiplier
I	10	20 m/min	40% and 20%[3]
II	9	20 m/min	40%
III	8	20 m/min	40%
IV	7	20 m/min	40%
V	10	20 m/min	100%
VI	10	20 m/min	10%
VII	6	20 m/min	40%

Table 3.2: Winding speeds

3.3.3 Capturing and weighing of resin losses at winding eye and spreader

In cases of significant dripping of resin during winding, the approximate resin ”losses” were determined by capturing the dripping resin on plastic sheets below the winding carriage while winding, peeling them off when cured, and weighing them. The setup is shown in figure 3.4.

During curing, the mandrel was kept rotating to prevent any local accumulation or dripping from rings that were over saturated with resin.

3.3.4 Weighing rings

Wound and cured rings were separated from each other and then weighed[4]. A dry ring was also wound, to determine the fibre weight fraction of a ring. In conjuction, the intention

[4]when possible. Cylinder I and II were joined together to such a degree that rings had to be sawn apart

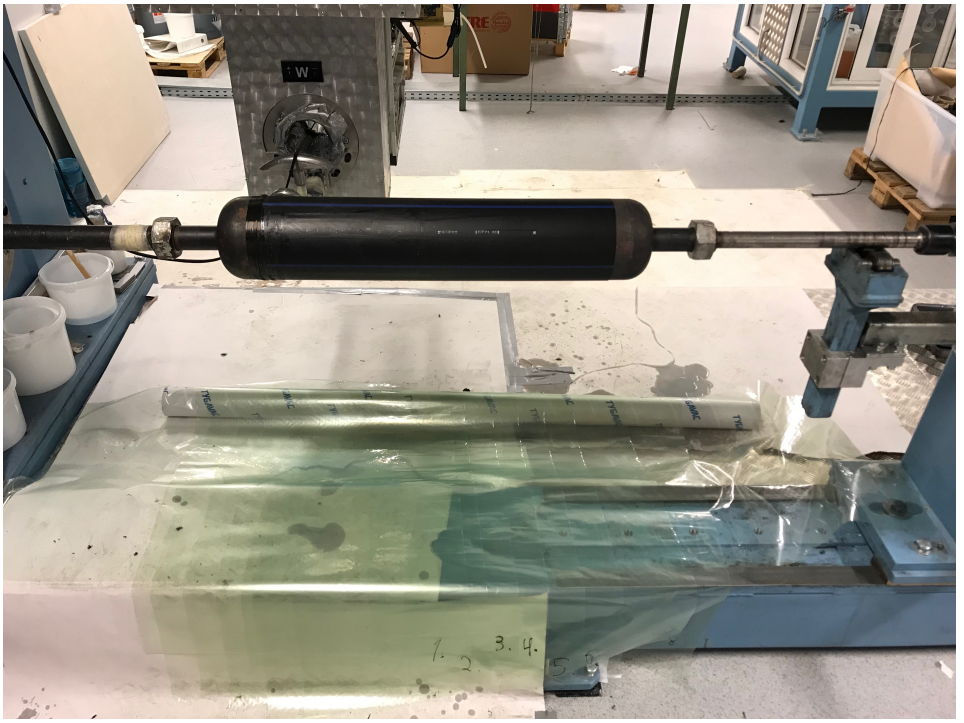

Figure 3.4: Sheets under the winding eye and spreader, removed after each ring finished winding.

is to determine the netto ring resin weight by subtracting the fibre weight from the various ring weights.

3.4 Specimen cutting and preparation

After winding, the process was as follows:

- The composites were cured for 24 hours at room temperature, while the mandrel was kept in rotation.
- Rings were loosened from their mandrel after winding and curing by freezing for a minimum of 3 hours. This shrinks the PE mandrel.[5]
- Cutting was done with a tomographic cutting machine, using an aluminium silicate blade running at 2750 rpm. This left a surface with relatively little roughness.
  - Water cooling was used for the entire cutting process.
  - The width of the specimens was controlled by a fixture during cutting, while the length was marked with calipers and thereafter cut ”by eye”.
  - Cylinders were cut first into rings, and subsequently the composite rings were post-cured in an oven at $80\,^{\circ}\mathrm{C}$ for $16\,\mathrm{h}$.
  - The rings were cut into circumferential segments, then from the centre of each segment the actual specimen was cut.
  - To prevent any possible moisture induced weakening of the composites from the water cooled saw, all specimens were placed in an oven at $80\,^{\circ}\mathrm{C}$ for a duration of at least $2\,\mathrm{h}$ after cutting.

Figure 3.5 shows specimen extraction and nomenclature as used in this report.

3.4.1 Microscopy

Microscopy samples were taken from the leftover material after specimen cutting. The initial surface left by the tomographic cutting process was refined by further polishing, down to 2000 grit paper.

3.5 Testing

3.5.1 Short beam shear testing

Specimen thickness, width and length were measured with a digital vernier caliper to the closest $1/100\,\mathrm{mm}$. The length was measured as the inner chord length, according to ASTM2344[17]. This is shown in figure 3.6.

ASTM2344 [17] provides details on the cutting process, layup, specimen dimensions and test setup The standard recommends a specimen length of 6x thickness, width of 2x

[5] The CFRP, with its low thermal expansion coefficient, stays very stable.

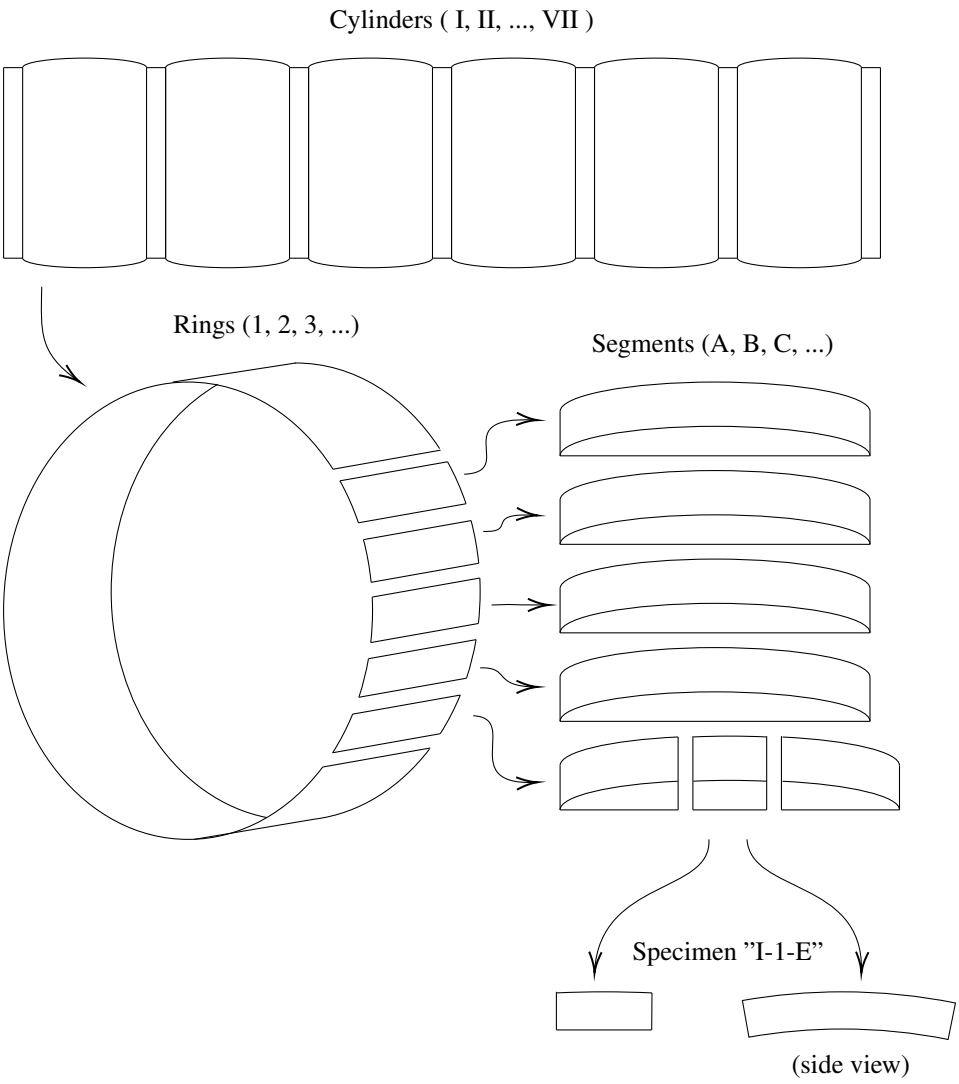

Figure 3.5: Overview of specimen extraction and nomenclature as used in the rest of the report

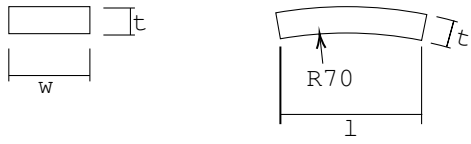

Figure 3.6: Short beam shear specimen dimensions

thickness and span width of 4x thickness. These recommendations were followed for a nominal composite thickness of $6\,\mathrm{mm}$.

The span width L was set to $24\,\mathrm{mm}$. This span would match a nominal thickness of 6mm. The composite was measured to be slightly less thick than this, but a nominal thickness of 6 mm was assumed so that the support span was became slightly larger, as the burr and edges of the specimens nearly touched the support fixture.

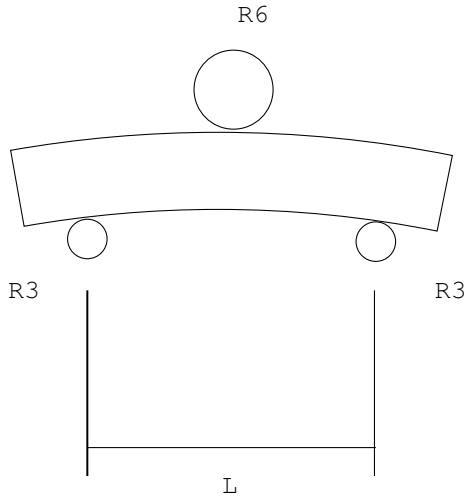

Figure 3.7: SBS test fixture setup

The sample size was 5.

Visible delaminations were noted and informed an aggregate presented in 4.7. Some specimens were painted in an attempt to increase the visibility of cracks that appeared. This was useful for photography but deemed unnecessary for the remainder of the speci-

mens as delaminations were found to be observable by the naked eye to a sufficient degree.

3.5.2 Determining fibre volume fraction

Carbon fibre is not suitable for a burn-off test as the mass of fibre itself is affected by the process. The choice of carbon fibre for this study restricts the use of burn-off as a method of determining volume fraction. Instead, entire rings have been weighed and compared to the weight of a similarly wound ring in a dry state, without any resin.

Literature is not consistent on the way of determining composite volume fractions. Burn-off and chemical etch based test will result in a ration influenced by the layer of neat resin that covers an ordinary composite, while analysis of cross-sectional fibre and resin area using microscopy will not be influenced by this and present a local volume fraction.

The ”ring-weighing” method used in this report shares the characteristic of the burn-off test and will result in values representing the resin fraction of the composite throughout its entire thickness, including the layer of neat resin.

Chapter 4

Results and analysis

Quantitative and qualitative data of interest is presented in a processed form in this chapter, and discussed in section 5. Other data, including all of the unprocessed data may be found in the appendix.

4.1 Overview of experimental work

[1]

196 specimens from 42 rings across 7 cylinders were wound and cut over the course of this study. A further 15 rings from these cylinders were wound at a dosing rate so low that it left the material too frail to cut and test, as it disintegrated in the process.

Some of the successfully wound material was intended for testing of other mechanical properties and is not used in this study.

Dosing rates ranged broadly from the level where the composite barely hangs together, to the point where most of the resin is very clearly being lost before it even reaches the mandrel, and the composite is visually clearly saturated, with much of the resin laying on top.

The steps however are not evenly spaced, more winding was done in areas that seemed interesting or out of practical reasons with what was easiest to do with the pump and silicon tube combination.

Cylinder I and IV make up the main investigation, presented in 4.3, detailing the progression of the short beam strength with increasing dosing rate.This ”curve” was put together over these two winding sessions as not enough dosing levels could be produced in a single winding session, given the desired resolution of this curve. The main limiting factor

[1] This can also be interpreted as the ”contributions” section often expected for a Master’s thesis

Cylinder nr.	Nr. of rings.	Base speed	Speed multiplier	Cylinder description and comments
I	10	20 m/min	40% and 20%	First (and drier) half of "normal speed" rings. Together 14 points make up the dosing rate vs. ILSS curve.
II	9	20 m/min	40%	Pot life comparison for 3 groups (1h, 2h, and 3h of expired pot life) of 2 rings, plus a third ring for ensuring against and analysing transients.
III	8	20 m/min	40%	Failed continuation of "normal speed" curve, post-winding rotation was interrupted and excess resin accumulated on a single side of the mandrel
IV	7	20 m/min	40%	Second (and wetter) half of "normal speed" rings. Together 14 points make up the dosing rate vs. ILSS curve. "Manual pulsing" (power on/off) was introduced at this point.
V	10	20 m/min	100%	Winding with a high fibre speed to see if this affects resin loss and impregnation quality.
VI	10	20 m/min	10%	Winding with a very low fibre speed to see if this affects resin loss and impregnation quality. Winding occured on a particularly hot day and pot life was reached before winding finished. No repeat winding could be done in time for this study.
VII	6	20 m/min	40%	Winding 4-layer rings for split disk testing. A different fibre (Torayca) was used.

Table 4.1: Overview of wound material

was the width of the available PE mandrels. Additionally, the dosing rate spanned a range that could not be covered by only changes in the pumping speed. Silicone tubes with two different inner diameters, 1.6mm and 3.2mm were used. Cross sectional areas between these tubes therefore theoretically differed by a factor of 4.

Cylinder II was produced to investigate the effect of pot life on the dosing rate and composite strength, and to see whether transient effects (of changing from one dosing rate to another) could be observed.

Specimens from cylinder V representing winding at a very high winding speed have been tested but not discussed, and specimens from cylinders VI and VII, representing winding at a very low speed and split disk rings, respectively, were not tested and are available for future analysis.

These specimens were produced to further investigate parameter relationships besides the main relationship between impregnation level and SBS.

Even among the tested rings, much material remains, available for future investigations into characteristics such as for instance fatigue life.

4.2 Flow rate calibration results

Figures 4.1 and 4.2 show the flow rates reached with the $3.2\,\mathrm{mm}$ and $1.6\,\mathrm{mm}^2$ silicone tubes at different duty cycles and stages of expired pot life, according to the method described in section 3.2.

[2]Inner diameter

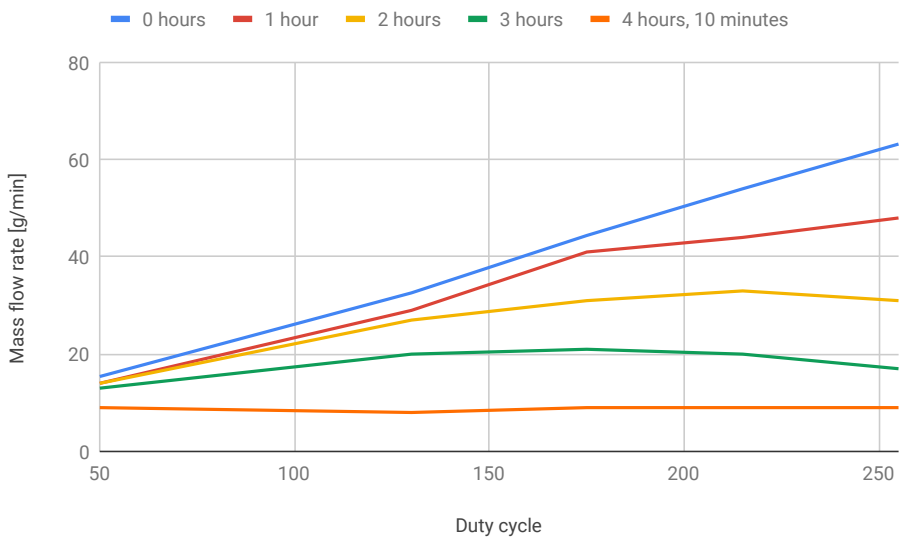

Figure 4.1: Flow rates measured with the 3.2 mm silicone tube at different duty cycles, for various stages of expired pot life

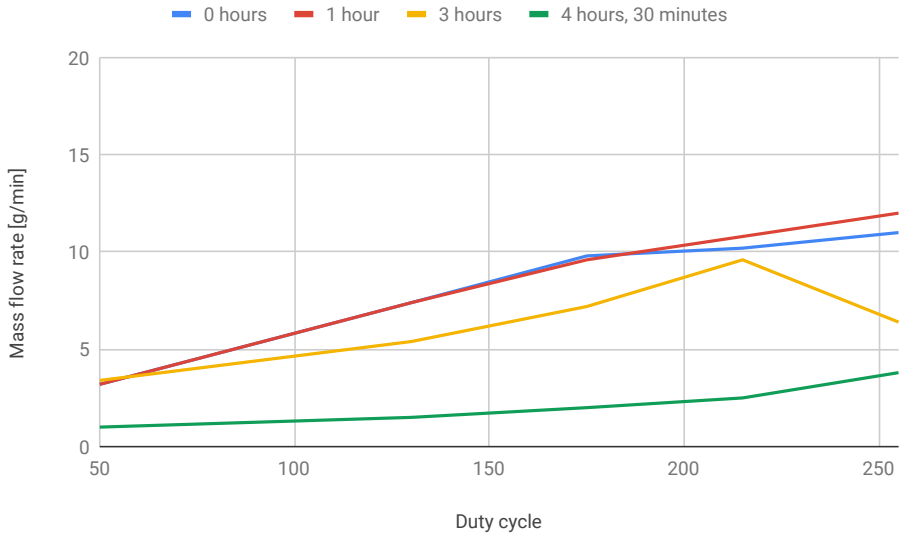

Figure 4.2: Flow rates measured with the 1.6 mm silicone tube at different duty cycles, for various stages of expired pot life

4.3 Short beam shear test results

All strength testing was done with a sample size of 5. Data for every specimen may be found in the appendix.

Figure 4.3 shows the strength vs. dosing rate for specimens from the ”normal speed” cylinders I and IV. The dosing rate is estimated by looking at the time difference from when resin was mixed, until when each ring was wound, and using the nearest calibrated values to estimate the mass flow rate. This dosing rate is an estimate of what was actually pumped out of the siphon during winding of that ring.

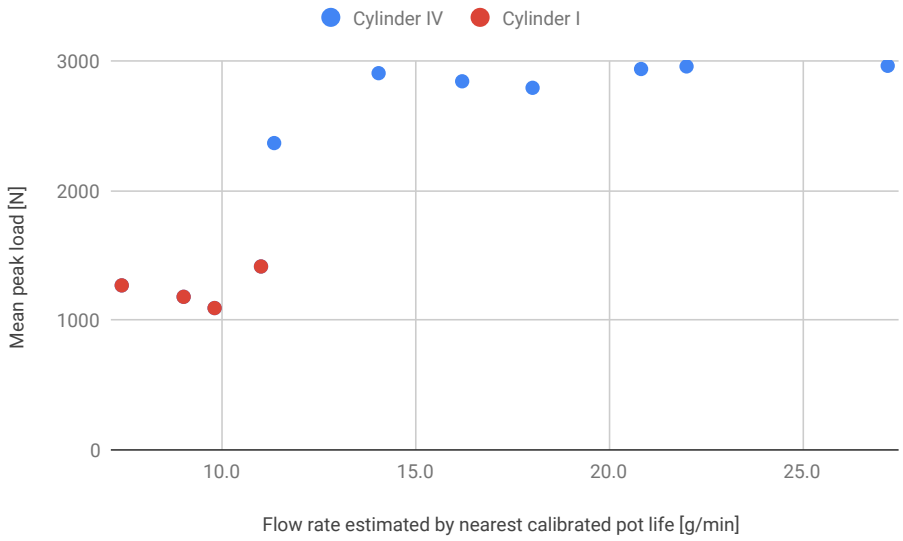

Figure 4.3: Strength vs. dosing rate for specimens from cylinder I and IV, wound at normal speed.

Figure 4.3 shows the strength vs. *impregnation rate* for specimens from cylinder I and IV. The impregnation rate is estimated by dividing the ring resin weights (obtained as described in section 3.3.4) over the measured winding time for the ring. This impregnation rate represents the rate at which resin actually reaches the composite, disregarding losses. Ring weights were not available for the data points from cylinder I, but losses for those rings are estimated to be entirely negligible, based on observations presented in section 4.6.

Figure 4.5 shows the strength vs. dosing rate for specimens from cylinder II, wound at identical duty cycles at two stages of expired pot life. The second and third dosing rate are nominally the same, but impregnation rate for the third ring was expected to be closer to steady state compared to the second ring.

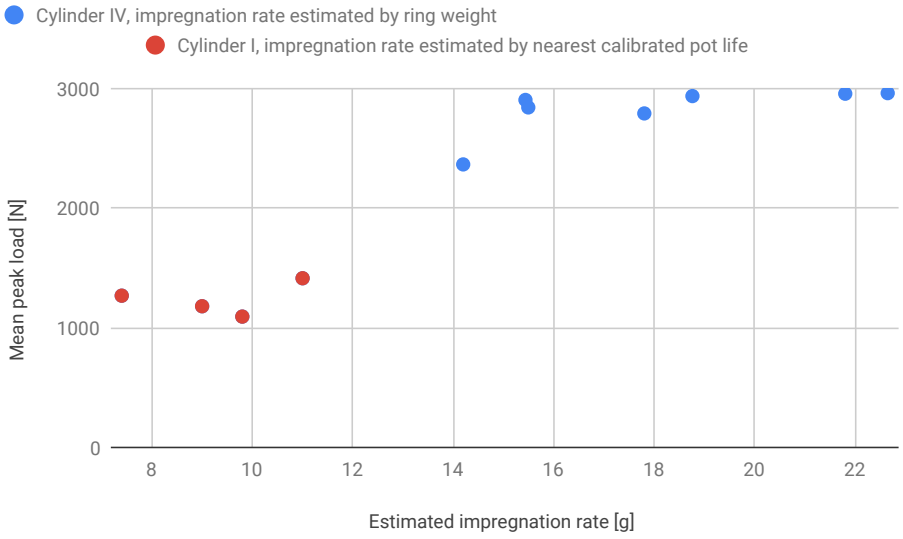

Figure 4.4: Strength vs. *impregnation rate* for specimens from cylinder I and IV, wound at normal speed.

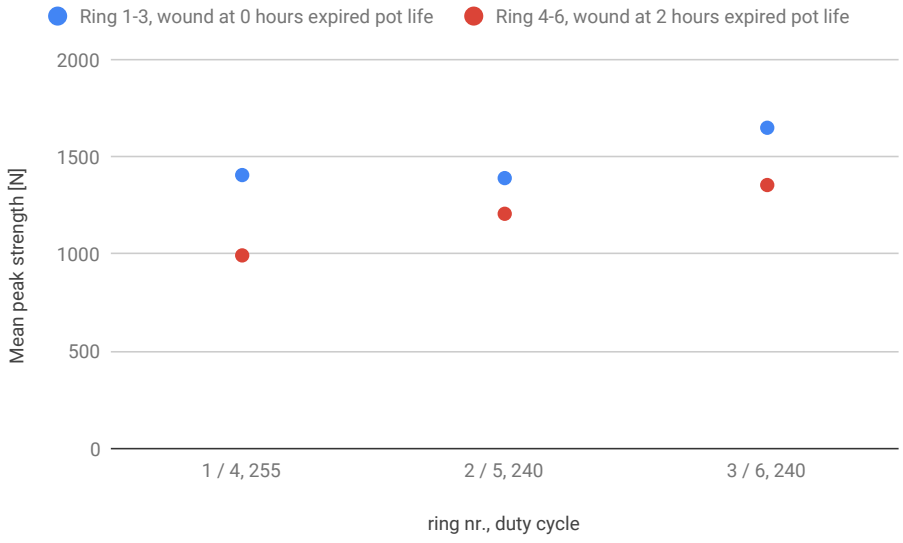

Figure 4.5: Strength vs. estimated mass flow rate for specimens from cylinder II, wound at identical duty cycles at two stages of expired pot life

4.4 Thickness development

As cylinders I and IV covered the largest spectrum of dosing rates, a progression of the average thicknesses from these cylinders is shown in figure 4.6. These are specimen thicknesses, measured as described in section 3.5.1.

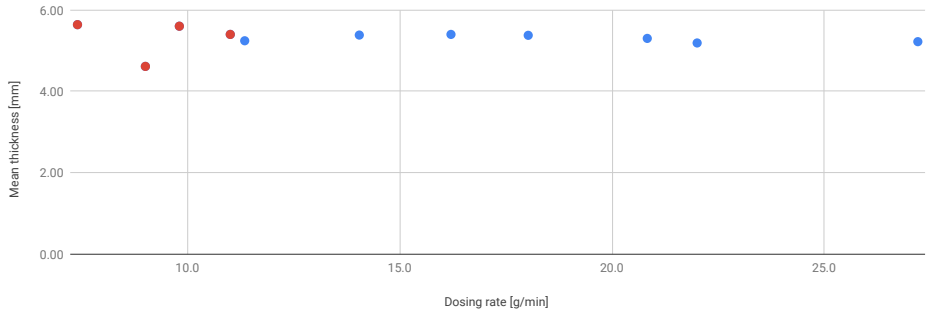

Figure 4.6: Measured thickness development with increasing dosing rate for specimens from cylinder I (red) and IV (blue), wound at ”normal speed”.

4.5 Resin accounting

By integrating the resin dosing rate over the ring winding time, the *estimated* total dosed resin can be found. By subtracting the measured resin losses, and comparing to the measured netto[3] ring weights, the possibility and accuracy of simple resin accounting can be investigated. Figures 4.7 and 4.8 show this comparison for cylinders V, and IV. cylinders for which both resin loss and ring weight data were available. Cylinder IV was wound 2 hours into the pot life, while cylinder V was wound immediately after resin mixing.

4.6 Observations during winding and specimen preparation

No leaking was observed from the siphon during winding. Although resin capture was not yet thought of when winding cylinder I and II, it was observed that there were barely any losses at the winding eye and tow spreader during these winding sessions. The few drops that were observed are estimated to make up a few grams in total. For those rings where significant dripping did occur, the amount of dripping at the winding eye was observed to be much higher than at the tow spreader.

Composites that were poorly impregnated are not commonly described in literature. The following section describes the progression of some composite characteristics, as the dosing rate ranges from dry to wet.

[3] ring weight minus the weight of a ring of dry fibre

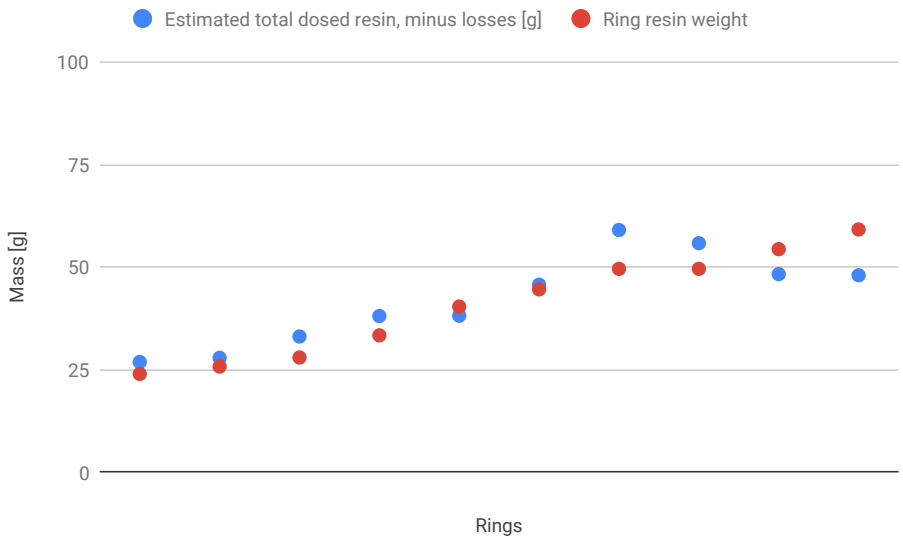

Figure 4.7: Comparison of netto ring weights and estimated total dosed resin for cylinder V

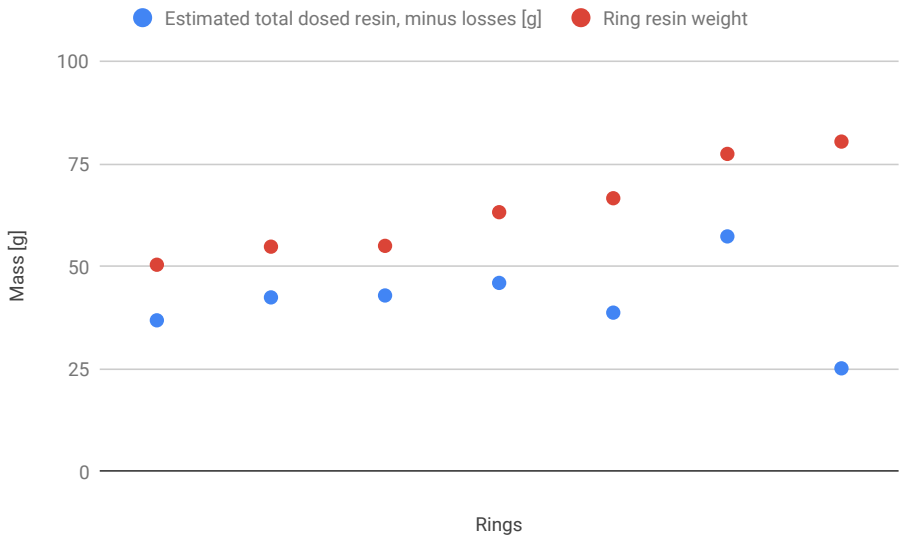

Figure 4.8: Comparison of netto ring weights and estimated total dosed resin for cylinder IV

- Initially, the composite has a completely dry outer appearance with no shiny surface resin at all. The aligned filaments are clearly distinguishable. Cutting specimens leaves filament ”bundles” near the top and bottom of the specimens as shown in figure 4.9.

- Ring I 4 is close to the lower limit of composites that can be ”handled”. Multiple rings impregnated at around this level have disintegrated in the process of cutting or even removing them from the mandrel. Ring 2 and 3 from cylinder 1 fell apart completely, as illustrated in figure 4.10.

- Composites impregnated at this level also feel damp to the touch after going through the water cooled cutting process, clearly having absorbed the water.

- Further along come the first ILSS specimens that remain neatly shaped after cutting, without any ”bundles” sticking out.

- The next visible change is that a top layer of resin starts becoming apparent. It does not appear in an evenly spread out layer that begins thin and slowly becomes thicker. Rather it lays as strands or streaks of shiny resin with oblong patches or streaks of dry fibre which still look as initially described.

- Following this, an even layer of top level resin starts to become present.

- Above this it is difficult to observe any changes.

  There is also a visible progression on a microscopic level. Micrographs of some specimens from cylinder I are shown in figure 4.11. Ring 9 on cylinder I was wound at the same dosing rate but half the winding speed compared to I8. This effectively doubled the dosing rate.

The bottom of specimens appears to look the same regardless of the impregnation level.

4.7 Qualitative SBS test results

Specimen failures had some characteristics in common. Image 4.12 is representative for the progression of a typical specimen failure.

For each specimen the crack development has also been denoted in a rough sketch. In aggregate these informed the idea of a ”typical” specimen failure, which has been sketched in 4.13.

- Within the first few seconds of loading, a faint crackle can be heard as the top layer of the composite suffers minor local compressive damage directly under the loading nose. This ”settling” process makes up the curved section at the start of the load-displacement curve. Deformation continues with linear elastic deformation until the peak load is reached, at which point one or more tiny delaminations occur at the edge of the specimen.

Figure 4.9: Appearance of a dry composite after cutting

Figure 4.10: A poorly impregnated composite left completely destroyed by the cutting process

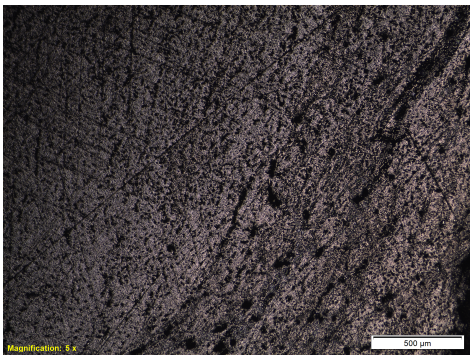

(a) Micrograph of a specimen from ring I2

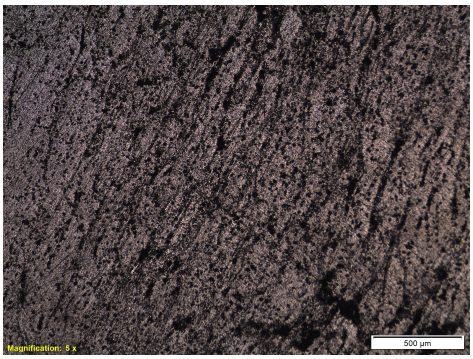

(b) Micrograph of a specimen from ring I5

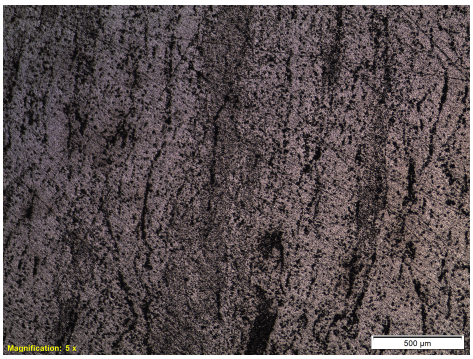

(c) Micrograph of a specimen from ring I8

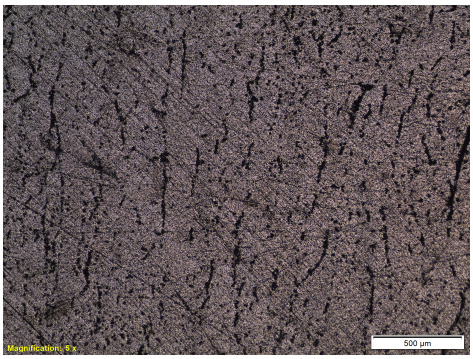

(d) Micrograph of a specimen from ring I9.

Figure 4.11: Micrograph of specimens from cylinder I. (a, b, c and d are in increasing dosing rate)

.

- These delaminations are accompanied by an audible clicking sound and a small drop in the load-displacement curve. In the case of these smaller scale delaminations, the sound is what initially reveals the delamination, and only after a few seconds do they become visible to the naked eye on the edge of the specimen.

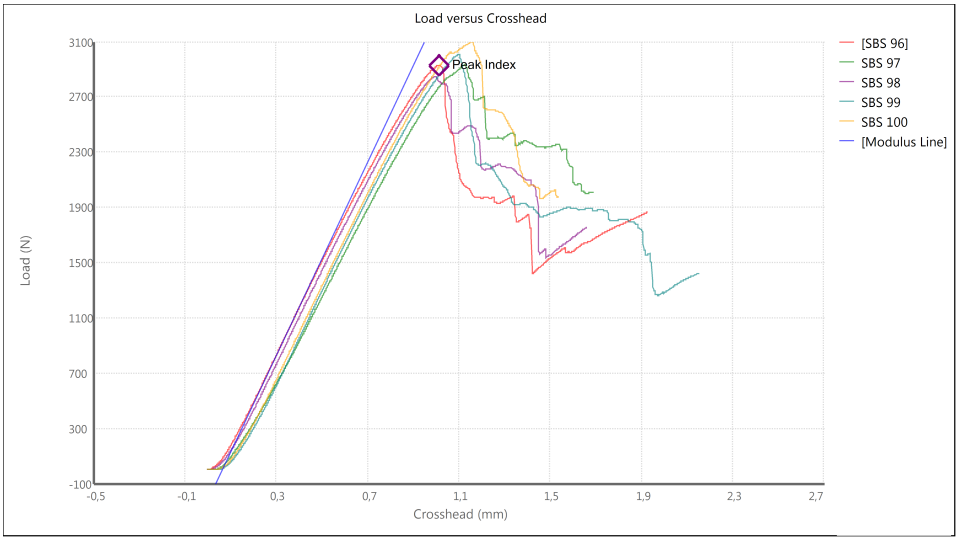

Figure 4.12: An illustration of some typical load-displacement curves during specimen loading and failure. The shapes are representative, the values will differ between samples.

- The curve continues to fall with numerous tiny delaminations, with the loading increasing slightly between each before falling to an even lower level. This continues until a major delamination occurs - either a seemingly new one occurring centrally in the specimen, or the sudden growth of one of the edge delaminations towards the centre. This point can be seen near the 1.5mm crosshead displacement mark on the curve for SBS 96 in 4.12.
- The edge delaminations that appear in numbers are usually created in a cascading effect, where one crack is followed nearly immediately by the rest. These create a distinct crackle sound and can be identified on the load-displacement curve by a staggered drop in loading, with many small decreases.
- The strongest sound and steepest, furthest drops in the load-displacement curve are associated with a single delamination that stretches from the edge to the interior of the specimen. Specimens with better impregnation can take higher peak loads but seem to reach these with less displacement, meaning they are stiffer. The load-displacement curve for these specimens also seems to have a longer ”tail” - they can resist a higher load after initially shearing. In a few cases this even went as far as being able to take a higher load after the first shearing event.
- Delaminations that extend into the horizontal centre of the specimen frequently occur at approximately one third to one fifth from both the top and the bottom, as

shown in figure 4.13.

Figure 4.13: Appearance of cracks in a typical specimen after failure.

Chapter 5

Discussion

5.1 Introduction

Discussion and conclusions will be made regarding the results both at they pertain to this composite in particular, and the optimization process in general. Emphasis in the discussion will be on the optimization process and considerations of using electronic resin dosing to optimize composite characteristics.

As noted in section 4.6, no resin was observed to be leaking from the siphon at any point during winding. The conditions for assuming a black box model of the impregnation chamber stated in chapter 2 are thereby upheld.

5.2 Dosing rate optimization

5.2.1 Presence of a transition zone

Both figure 4.3 and figure 4.4 appear to indicate that there is a flat region on the dry end of the spectrum, reaching up to about 10 g/min, where specimens remain weak despite the introduction of more resin. Both curves also feature a point after which the ILSS roughly stays the same. This point lies around 15 g/min. Between these two flat regions, a transition area can be found.

The data for this curve had to be produced over two cylinders, as one mandrel was not wide enough for the number of rings to be produced. Each session also covered the entire range of 1 of the silicone tubes.

The specimens from cylinder I were wound with the rings close enough together that they overlapped in sections. Specimens were extracted from appropriate sections on the rings, but the differences in winding setups between I and IV could potentially have displaced the SBS values to produce a larger gap between the two datasets that make up the curve. However, within each of the halves the tendency of SBS vs dosing rate curve can also be observed and there is clearly a trend towards a transition in the end of I and the beginning of IV. Visually, this is also the area of transition to saturation.

5.2.2 Mechanism

Given that the degree of wetness changes so significantly from the lower end to the higher end of the spectrum, there is a surprising consistency in the thickness among specimens from the various rings. Even when there is a clear visual change in surface quality from the dry-fibre-like appearance to the shiny and smooth specimens, there is virtually no change in thickness. This hints at the fact that it is the void fraction that is most subject to change as the dosing rate changes.

This is also evident from the microscopy results presented in figure 4.11.

5.2.3 Pot life and transient investigation

The intentions of the test of cylinder II, whose results are shown in figure 4.5, were to see the direct influence of pot life on the composite strength, and to investigate the significance of transients as conceptualized in figure 2.7 in section 2.

For the former, results clearly demonstrate that unless the pot life effects are compensated for, the strength of the composite will suffer over prolonged winding sessions. For constant nominal dosing rates, the real dosing rate will be reduced with increased pot life and viscosity, leaving the composite drier than intended. This is directly reflected in the strength, as has been established in section 5.2.1.

Regarding the latter, cylinder II was found to be much too dry to be useful for the intended analysis of transient effects. As discussed below in the section 5.3 on uncertainty, it is clearly that at the dry end of the spectrum, the spread is so large that any comparative studies done in that range are of limited value. The effect of transients in this case seems to be much smaller than any variation in the results and it is therefore not possible to say how significant these have been. However from a theoretical consideration, given the size of the rings to be wound and the size of the siphon used, if the dosing rate were to be changed from maximum flow rate to an absolute minimum, the largest effect a transient could have is equal to the volume of the puddle in siphon, for example 5 mL, spread over the netto resin weight of the ring, for example 50 g. In this extreme case the deviation from the intended dosing rate would still only be approx. 10%.

5.3 Experimental uncertainty

There seems to be a larger spread in strength results among the low dosing rate specimens. Within samples, values for peak load are in accordance with each other even though the displacement at which they are reached can differ slightly. Statistical data may be found in appendix C1.

5.3.1 Specimen preparation and cutting effects

Influence of moisture

Water cooling has kept the resin from reaching too high temperatures during the cutting process but water ingress has been shown to weaken composites. Post-curing at $80\,^{\circ}\mathrm{C}$

degrees for 16 h after cutting is assumed to simultaneously have evaporated any significant traces of water in the composite.

Moisture weakening in normally impregnated composites is usually significant only after long term exposure. [18] shows that moisture uptake after exposure shorter than a day, remains below 0.1 wt.% for a properly impregnated composite. A maximum of approximately 0.6 wt.% is reached after 1 month of exposure. At this level the ILSS strength was shown to be reduced by 20%.

However, specimens that are not fully impregnated will absorb moisture to a much higher degree, to the point where the composite can feel damp to the touch for a long time after exposure. The effect on such poorly impregnated composites is again unknown, and so extra drying in an oven was done as a precaution.

5.3.2 Testing uncertainty

Manual stopping of test, not in accordance with ASTM234. The stopping conditions for the strength testing machine were not implemented and stopping was therefor done manually by the operator. This is not in accordance with ASTM D2344. as mentioned in section 4.7, in a few cases this even went as far as being able to take a higher load after the first shearing event. This might upset the sample spread, as other specimens in the sample were not allowed to continue to that level.

There was a clear bias towards fraying type of delaminations on one side, indicating an off centre loading. It is very difficult to get loading centered so precisely that the side of failure is arbitrary,

5.3.3 Issues with standard ASTM2344D

Discussion of standard ASTM2344 SBS test itself The short beam shear test results in a complicated stress situation in specimens that is hard to tie directly to a single mechanical property. [19]

However, the standard is not designed for poorly impregnated composites, and as this is a comparative study, the results are still valid in revealing differences in dosing rate.

5.4 Flow rate calibration

Figures 4.1 and 4.2 clearly show that flow rates change with expiring pot life. In both the case of the 1.6mm tube and the 3.2 mm tube, the results for 0 hours and 1 hour are very similar to each other. After that, changes in viscosity change the relationship between the duty cycle and the mass flow rate, likely because of the increased flow resistance throughout the silicone tube through which the resin is pumped.

If flow rates are to be calibrated only once with freshly mixed resin, the above results show that pot life need not be given much consideration as long as winding sessions remain shorter than 1 hour.

For sessions longer than this, calibration at multiple points in time will be required

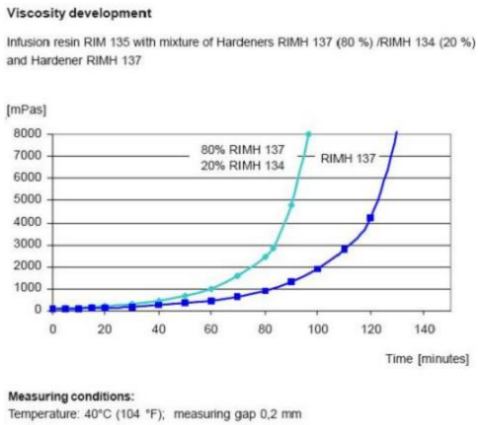

Figure 5.1: Viscosity vs time development from the Hexion RIMR 135 datasheet.

unless significant changes are made to either the resin dosing hardware or winding procedures (such as using a static mixer[1] so that resin is always freshly mixed).

Dosing rates established by calibration can be extended to in between values of pot life and duty cycle by means of interpolation.

The calibration results also make clear that even while the manufacturers stated pot life may be a valid estimate of the ”working life” of the resin, pot life alone is not a useful metric when used in conjunction with resin dosing systems.

The Hexion RIMR 135 datasheet, shown in figure 5.1, contains a viscosity vs. time curve that agrees with the initial flat viscosity development noted above.

As the temperature for this datasheet was $40\,^{\circ}\mathrm{C}$, and viscosity and pot life are heavily temperature dependent, values in this graph were not further applicable for winding and dosing at around room temperature.

All winding experiments of interest could be performed using the 1.6 and 3.2 mm tubes. Given that the machine supports one size lower (0.8 mm ID) and a size larger (4.8 mm ID), the pump is aptly dimensioned for the purposes of the NTNU composite lab when considering the typical winding speeds employed.

Furthermore, given the availability of these tubes, there is ample room for increasing the flow rate further for experiments with for instance multi-tow impregnation (although the siphon is not built for this) or even higher winding speeds, or reducing it to have more fine grained control.

5.5 Importance of pot life and viscosity

The resin accounting results presented in section 4.5 show clear differences in the accounting accuracy for cylinder V and cylinder IV. The capture and measurement both

[1] A long baffled tube which intimately mixes two component resins by repeatedly splitting and merging the stream.

resin losses and ring weights are both assumed to be relatively accurate processes, as the measurements are made directly and resin cannot simply disappear.

For this reason, it is the third factor, the estimated dosing rate, which likely throw off results for cylinder IV. In light of the fact that cylinder IV was wound 2 hours into its pot life while V was wound immediately after mixing resin, this hints at the uncertainty that pot life and viscosity adds to the resin dosing process.

If pot life and viscosity were not independent of other factors, calibration would only have to take place once to generate data for all subsequent winding with that resin. However this is not the case. The failed winding of cylinder VI was caused by the pot life being accelerated by the influence of hot weather, to the point where the pot life was actually reached after approximately 3.5 hours and the remainder of the resin in the reservoir was fully hardened. The surface of this cylinder also exhibited amine blush, likely due to the accompanying high humidity[14].

Similarly, the calibration of the 1.6mm tube was done on a particularly cold day, and figure 4.2 shows pumping to continue to 4.5 hours and beyond.

As shown by the abovementioned results and discussion it is therefore not just the pot life by itself but the interdependence of pot life and other factors such as those described in chapter 2 that complicate resin dosing.

This is what has necessitated repeated calibration of flow rates throughout this study.

The results from the winding of cylinder II, presented in 4.5, also show that that if nothing is done to compensate for the pot life progression, the strength of the composite will suffer.

5.6 Resin waste and optimization of resin consumption

The largest wastes of resin come from the resin losses dripping from the winding eye and tow spreader. These are also complicating the estimation of how dosing rates influence the mechanical properties, but as shown in 4.7 this can to a significant degree be compensated for with simple resin accounting. One cannot ”compensate” for losses in a way that winding happens without any losses, losses are to some degree part of every possible setting on the pump, with otherwise normal winding equipment.

But these surfaces could be replaced with some enclosed surface similar to the siphon impregnation system, or potentially even removed. The effectiveness of the siphon by itself (without the subsequent spreader and winding eye) has not been investigated during this study or by [4], but it could be sufficient to get appropriate impregnation.

A siphon is mechanically different from the spreader and winding eye as the resin that is ”scraped off” actually ends up back in the pool in the siphon, such that it acts as a stable system to a certain degree, where the same amount of resin leaves the siphon as enters it, so that the exact amount which ends up on the tow can be known, in spite of ”massaging” things properly. Each surface then acts as it’s own ”black box” where resin gets locally ”recycled”. This can reduce resin consumption and increase the predictability of resin dosing, but fluffs anecdotally seem to be more of an issue and friction could potentially increase.

Optimizing *the amount of resin used* is not the same as optimizing the amount of resin *present on the mandrel*. Reducing the first can be done by reducing waste throughout the

production process in the way described above. The second requires closer inspection on the effect of reducing impregnation level on the mechanical properties of the composite. Optimizing the amount of resin present could reduce the weight of for instance a pressure vessel with an acceptable hit to the mechanical properties under consideration.

5.7 Limitation of chosen scope

Other properties are also of importance:

- Impact is of particular importance to composites that are subject to transport and handling, such as pressure vessels.
- Fatigue life is also a property of great importance since pressure vessels experience pressure cycling as they are repeatedly filled up and emptied.

Impact and fatigue testing were both outside the scope of this study but the filament wound material is available for further research.

Different fibre can give different specific results for the impregnation vs ILSS curve because of physical/geometric properties, such as size etc. but also the effect of a different sizing.

The stiffness is also changed with dosing rate, but only strength has been considered. Stiffness characteristics can be gathered from the curves presented in the appendix.

Chapter 6

Conclusions

6.1 Summary of findings

- Results initially confirm that the newly developed prototype for computer controlled resin dosing is able to impregnate composite rings to various degrees.

- Pumping resin under tightly controlled conditions such as when calibrating freshly mixed resin confirms that the pump system by itself provides repeatable results. However environmental factors such as temperature and humidity complicate the dosing accuracy some time into the pot life.

- Disregarding uncertainties caused by the pot life, simple resin accounting by the capturing of spilled resin has been shown to work and to be effective in estimating the rate of impregnation the composite is actually subject to.

- Results indicate that there is a distinct transition zone of increasing short beam strength as the dosing rate moves from approximately 10 g/min to 16 g/min. On either side of this zone, the strength largely remains flat.

- An accurate, quantified judgement on the waste improvement over the previous system can not be made as no numbers exist for resin consumption with the traditional system. Qualitatively it is known that dripping commonly took place and layers of excess resin were always removed from the mandrel by hand scraping during a winding session. If this is no longer necessary for an operator using the settings determined by this study, it can be stated that resin consumption resulting from the current work is significantly lower than earlier.

- This experiment with SBS values can serve as an example of the kind of parametric study that can be done with the precision dosing, repeatability, and variable control offered by electronic resin dosing and closed impregnation filament winding. The

exact same can be done for other parameters, such as tensile strength. The considerations and findings regarding around winding precision, resin dosing precision and cutting are relevant for and can be extended to other mechanical tests.

- The biggest contributor to the uncertainty are the viscosity and pot life, and the way these depend on environmental conditions.
- Getting control over or modelling these would be beneficial, and subject to further work.
- With further improvements, this procedure can form the basis for a straightforward and precise method that can be used by production facilities to optimize resin usage for their specific fibre, resin and other circumstances.

6.2 Further work

6.2.1 Testing other mechanical properties

Tensile testing

As tensile strength is the primary mechanical property of interest in the context of composite pressure vessels, some split disk tests should be done to ensure that this property is not sacrificed (lost in any significant way) in optimising based on interlaminar shear strength.

To get an impression of whether the tensile properties are sacrificed in any regard in the process of optimizing for interlaminar shear strength, a small number of specimens rings were wound for use in split-disk tensile testing. Split disk test results exist for the given resin system and fibre combination at this department, produced with the siphon and also the traditional drum impregnation system. With the introduction of the electronic dosing system, the split disk results can be compared to the former.

Split disk specimens have been produced for this purpose during this study, but testing is left to future work.

It is expected that the fibre direction strength will not be directly correlated with the dosing rate, but at very low impregnation levels the integrity of the composite ring could be compromised.

6.2.2 Principal component analysis

The interdependence of the various resin dosing factors makes a statistical approach such as principal component analysis worth trying.

Performing principal component analysis with a full factorial design might be too involving. A fractional factorial design such as done by [12] is relevant in this context as many of the contributing factors likely have common dependencies such as on temperature or remaining pot life. With the data from this study plus data on the dependence on other factors acquired from any future studies, a large enough dataset is available for principal component analysis to provide some interesting results.

To gather more data for the principal component analysis (PCA), the winding process can be outfitted with more instrumentation such as resin bath thermometers.

Bibliography

[1] Hexagon CNG cylinder, https://www.hexagon.no/prod_images/doc_293_1.jpg.

[2] Dip Tray Schematic, https://www.autonational.com/images/filament_winders/dedicated-winder/diptray-dwars.jpg.

[3] Drum Tray Schematic, https://www.autonational.com/images/filament_winders/dedicated-winder/drumtray-dwars.jpg.

[4] Mats Mulelid. Novel Impregnation System for Filament Winding. Technical report, NTNU, 2018.

[5] Raoul Pathak. Resin dosing for closed impregnation filament winding. Technical report, NTNU, 2018.

[6] DONALD ADAMS. The short beam shear test : CompositesWorld.

[7] A Miaris, M Päßler, J Lichtner, and R Schledjewski. "Siphon impregnation": The development of a new method for impregnation during filament winding. Technical report, Institut für Verbundwerkstoffe, 2009.

[8] A Filament Winder Buyer's Guide : CompositesWorld, https://www.compositesworld.com/articles/a-filament-winder-buyeramp39s-guide.

[9] Resin Baths - McClean Anderson, http://www.mccleananderson.com/index.cfm?pid=14&pageTit
Baths.

[10] Angelos Miaris. *Experimental and simulative analysis of the impregnation mechanics of endless fiber rovings*. Inst. für Verbundwerkstoffe, 2012.

[11] S. Tiwari and J. Bijwe. Surface Treatment of Carbon Fibers - A Review. *Procedia Technology*, 14:505–512, 2014.

[12] D. Cohen. Influence of filament winding parameters on composite vessel quality and strength. *Composites Part A: Applied Science and Manufacturing*, 28(12):1035–1047, 1997.

[13] Glenn O. Brown. The History of the Darcy-Weisbach Equation for Pipe Flow Resistance. In *The History of the Darcy-Weisbach Equation for Pipe Flow Resistance*, pages 34–43. American Society of Civil Engineers (ASCE), 11 2004.

[14] Amine blush when working with epoxy: what you need to know.

[15] Achieving Pulseless Flow in a Peristaltic Pump.

[16] Analyzing Control Systems with Delays.

[17] ASTM Standard. D2344/D2344M-16. *"Standard Test Method for Short-Beam Shear Strength of Polymer Matrix Composite Materials and Their Laminates", ASTM International, West Conshohocken, PA*, 2016.

[18] S G R Brown, J M Ryan, and R Adams. Moisture Ingress Effect on Properties of CFRP. Technical report, Materials Research Centre, School of Engineering, Swansea University, 2009.

[19] DONALD ADAMS. Can flexure testing provide estimates of composite strength properties? : CompositesWorld.

[20] bogde/HX711: An Arduino library to interface the Avia Semiconductor HX711 24-Bit Analog-to-Digital Converter (ADC) for Weight Scales.

Appendix

6.3 Appendix A: Prototype hardware overview

An overview of the prototype resin dosing system hardware is given in figure 6.1 and 6.2.

1. Siphon impregnation unit[1]
2. Verderflex EZ peristaltic pump
3. $20\,\mathrm{kg}$ aluminium load cell
4. Input for $15\,\mathrm{V}$ DC power supply . The dosing system may accept any DC voltage between $5\,\mathrm{V}$ and $15\,\mathrm{V}$, but the available torque and the dosing speed are directly influenced by the supplied voltage. Values are currently calibrated for the $15\,\mathrm{V}$ currently supplied, and will be different when using another power supply, requiring re-calibration.
5. L298N H-bridge. Switches the $15\,\mathrm{V}$ signal going to the motor, based on the PWM signal coming from the microcontroller
6. HX711 Load cell driver, containing a Wheatstone bridge and analog-to-digital converter (ADC). Polled by microcontroller at $10\,\mathrm{Hz}$.
7. Arduino Uno microcontroller outputs a PWM signal to the H-bridge with a duty cycle between $0\,\%$ and $100\,\%$, set by the user via a serial monitor.
8. Resin reservoir platform
9. Mounting bracket, using a Bosch Rexroth aluminum profile compatible with the profiles used in the Mikrosam winding machine carriage.
   (a) Connection provides height adjustment to accommodate the height of the tow, such that it enters the PTFE siphon without scraping along its edges.
   (b) Provides adjustment along the width of the carriage to accommodate the use of any of the 8 winding eyes available.

The entire assembly is mounted to an aluminium frame in such a configuration that the entire unit can be mounted from a single point, and such that any of the 8 winding eyes may be used without causing collision between the system and the surrounding carriage.

[1] Described in further detail in [4]

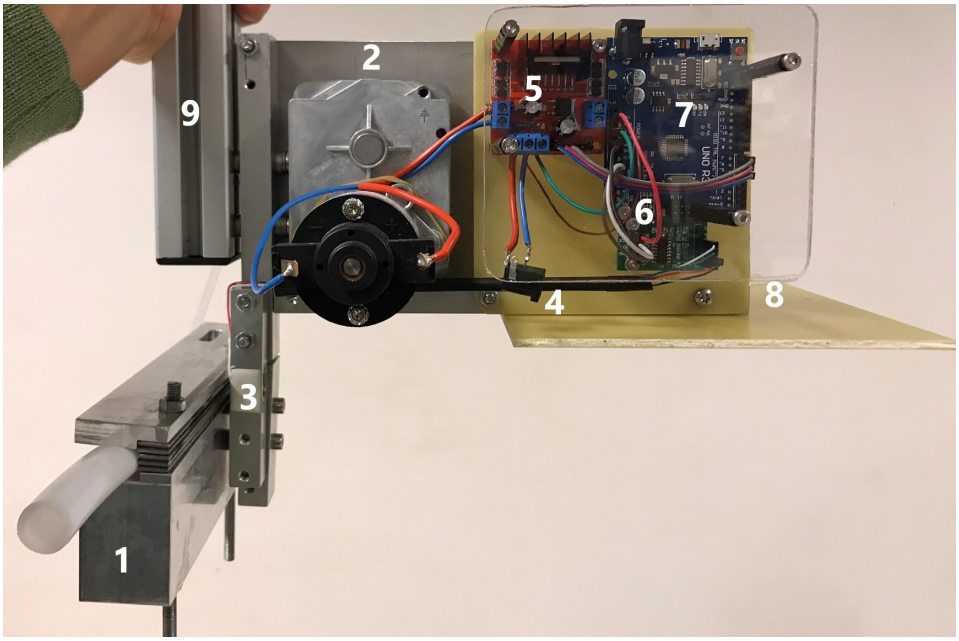

Figure 6.1: back view of resin dosing system

The load cell functionality was intended to measure frictional forces generated during winding, to see if these differed for various impregnation levels. This signal was subject to significant noise and machine vibrations [5] and the functionality is not used in this study.

For completeness, a sample of the load cell measurements together with the pumping speed is included in figure 6.3.

It shows the duty cycle [on a range of 0...255] along with the accompanying load cell readings [not directly related to physical units]. The horizontal axis shows the number of samples.

The noise in the readings is caused both by electrical noise affecting the sensor, and vibrations in the fibre tension system. The springiness of the pump and dosing system as it hangs from the winding machine carriage also brings vibrations, which might further contribute to the noise.

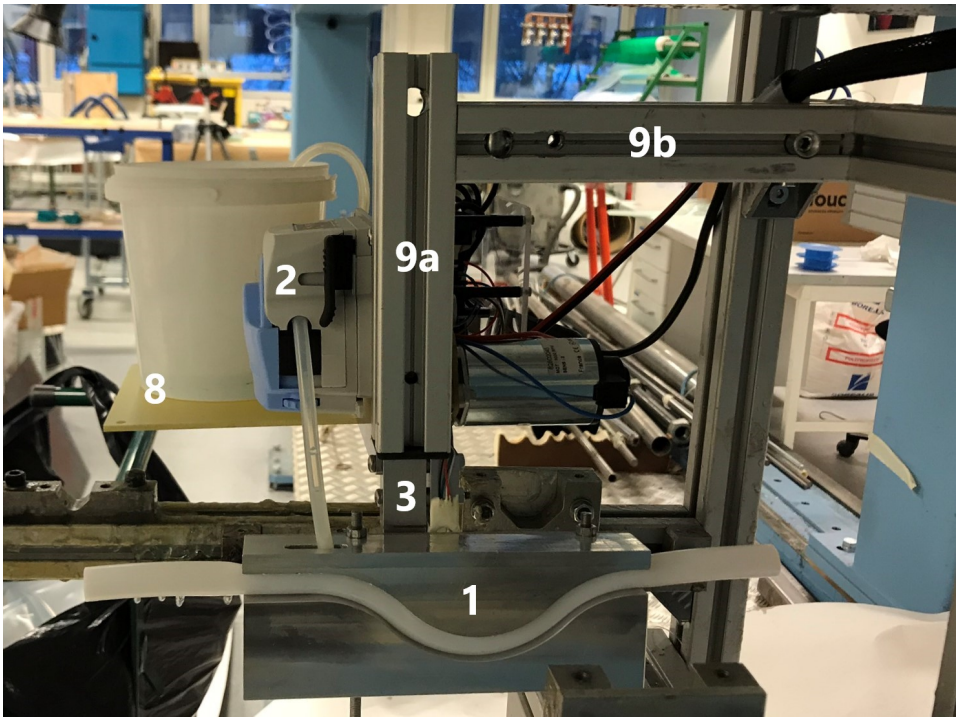

Figure 6.2: Side view of resin dosing system, as installed in the winding machine carriage

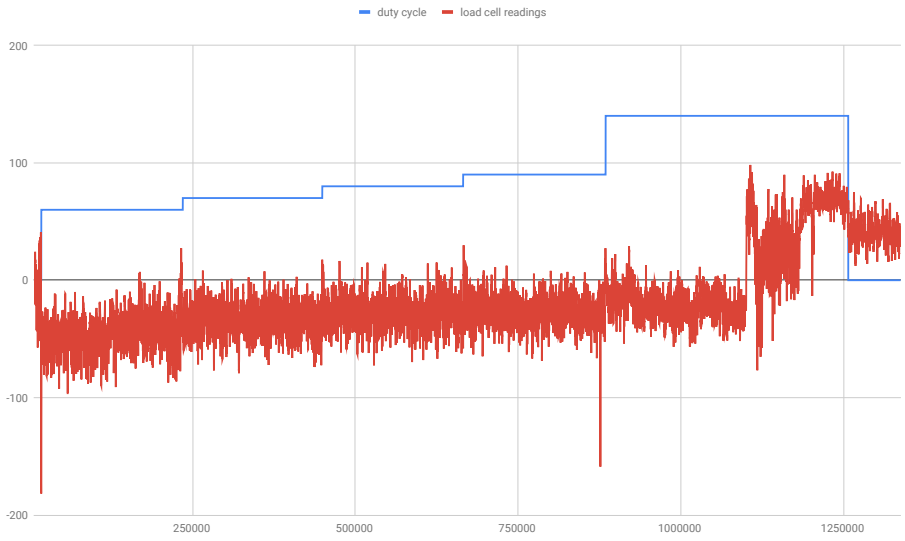

Figure 6.3: Load cell readings during winding

6.4 Appendix B: Code

Libraries used: HX711.h, licensed under MIT license. [20] The HX711 library and the lines of code that make use of it, are related to the load cell feature of the system which has not been used for this study.

```
#include "HX711.h"

#define enA 5
#define in1 6
#define in2 7

int receivedByte = 0;
int received = 0;
int dCycle = 0;
int count = 10;

HX711 scale;

void setup() {
  //Set up communication
  Serial.begin(38400);

  //Set output pins
  pinMode(enA, OUTPUT);
  pinMode(in1, OUTPUT);
  pinMode(in2, OUTPUT);

  // Set initial rotation direction, and zero speed
  digitalWrite(in1, LOW);
  digitalWrite(in2, HIGH);
  analogWrite(enA, 0); // Send PWM signal to L298N Enable
      pin

  //Setup of load cell:
  Serial.println("Initializing␣the␣scale");
  // parameter "gain" is omitted; the default value 128 is
      used by the library
  // HX711.DOUT  - pin #A1
  // HX711.PD_SCK - pin #A0
  scale.begin(A1, A0);

  scale.set_scale(2280.f);
  scale.tare();               // reset the scale to 0

  Serial.print("get␣units:␣\t\t");
```

```
39   Serial.println(scale.get_units(5), 1);        // print
       the average of 5 readings from the ADC minus tare
       weight, divided
40             // by the SCALE parameter set with set_scale
41
42   Serial.println("millis,duty␣cycle,load␣cell␣readings");
43 }
44
45 void loop() {
46   //Receive and parse serial data from Serial Monitor on PC
47   receivedByte = Serial.read();
48   if (receivedByte != -1) { //Serial.read() returns -1 when
       buffer is empty
49     while (receivedByte != 10) {//Look for ASCII new line
         feed character (10), signifying end of transmission
50       received = (received * 10) + (receivedByte - 48); //
           Convert ASCII char to integer with right exponent
51       receivedByte = Serial.read();
52       }
53     if (received >= 0 && received <= 255){ //limit range
         for accepted integers
54       dCycle = received;
55       //dCycle = map(received, 0, 100, 0, 255);
56       //Serial.print(millis());
57       //Serial.print(",");
58       //Serial.println(received);
59       //Serial.print(",");
60       //Serial.println(dCycle);
61       //analogWrite(enA, received);
62
63       analogWrite(enA, dCycle);
64       //delay(60000); //Uncomment these three lines for
           easier calibration
65       //dCycle = 0;
66       //analogWrite(enA, dCycle);
67       }
68     received = 0;
69     }
70
71   if (dCycle <= 100){
72     count = count + 10;
73     if (count > 100){
74       count = 10;
75     }
76     if (count > dCycle){
```

```
77        analogWrite(enA, 0);
78      } else{
79        analogWrite (enA, 130);
80      }
81    }
82
83    Serial.print(millis());
84    Serial.print(",");
85    Serial.print(dCycle);
86    Serial.print(",");
87    Serial.println(scale.get_units(), 1);
88
89    //scale.power_down();              // put the ADC in
          sleep mode. Not needed under normal circumstances
90    delay(100);
91    //scale.power_up();
92  }
```

6.5 Appendix C1: Ring parameters and average measurements

Table 6.1: Ring winding parameters

Ring	Speed [%]	Expired pot life	Estimated flow rate [2]	$\bar{w}$	$\bar{t}$	Mean ILSS[MPa]	ILSS
I 1	40	0:14:00	7.4	-	-	-	-
I 2	40	0:17:00	7.4	11.84	5.64	14.3	0.95
I 3	40	0:27:00	9	-	-	-	-
I 4	40	0:30:00	9	11.92	4.61	16.1	1.43
I 5	40	0:34:00	9.8	12.27	5.60	11.9	0.56
I 6	40	0:38:00	9.8	-	-	-	-
I 7	40	1:00:00	11	-	-	-	-
I 8	40	1:08:00	11	11.66	5.40	16.8	1.75
I 10	20	1:19:00	9.8	11.80	5.60	27.7	1.69
I 9	20	1:12:00	11	11.99	5.72	26.5	2.42
II 1	40	0:13:00	11	11.73	5.20	17.3	2.12
II 2	40	0:17:00	10.6	11.96	5.43	16.0	0.86
II 3	40	0:21:00	10.6	12.07	5.69	18.0	0.65
II 4	40	2:07:00	7.7	12.13	5.59	11.0	1.11
II 5	40	2:11:00	7.42	12.05	5.72	13.1	0.80
II 6	40	2:15:00	7.42	12.03	5.57	15.2	0.73
II 7	40	3:50:00	?	-	-	-	-
II 8	40	3:54:00	?	-	-	-	-
II 9	40	3:58:00	?	-	-	-	-
III 1	40	0:57:00	14	[3]	-	-	-
III 2	40	1:00:33		-	-	-	-
III 3	40	1:04:06		-	-	-	-
III 4	40	1:07:39		-	-	-	-
III 5	40	1:11:12		-	-	-	-
III 6	40	1:14:45		-	-	-	-
III 7	40	1:18:18		-	-	-	-
III 8	40	1:22:00		-	-	-	-
IV 1	40	1:48:00	11.34	11.28	5.24	30.0	1.98
IV 3	40	2:01:00	14.04	12.16	5.38	33.3	0.48
IV 4	40	2:05:00	16.2	12.08	5.40	32.7	1.04
IV 5	40	2:08:00	18.02	12.18	5.38	32.0	0.84
IV 6	40	2:12:00	20.825	12.27	5.30	33.9	0.97
IV 2	40	1:55:00	22	12.12	5.19	35.3	0.77
IV 7	40	2:16:00	27.2	12.16	5.22	35.0	1.56
V 1	100	0:17:00	21.4	12.22	5.06	21.5	1.44
V 2	100	0:19:00	24.8	12.34	5.04	25.0	1.59
V 3	100	0:20:00	28.6	12.05	5.16	30.0	1.30

[3] Specimens produced for 1st ring only, but not tested.

Table 6.1: Ring winding parameters

Ring	Speed [%]	Expired pot life	Estimated flow rate [2]	$\bar{w}$	$\bar{t}$	Mean ILSS[MPa]	ILSS
V 4	100	0:22:00	32.4	12.23	5.14	32.0	2.68
V 5	100	0:23:00	37.4	12.07	5.06	29.3	2.35
V 6	100	0:25:00	44	12.29	5.03	23.6	0.92
V 7	100	0:26:00	52	12.09	4.98	25.6	0.98
V 8	100	0:28:00	53.4	12.24	5.30	-	-
V 9	100	0:29:00	57.4	-	-	-	-
V 10	100	0:31:00	64.4	-	-	-	-
VI 1	10	-	-	11.36	5.16	34.3	1.49
VI 2	10	-	-	-	-	-	-
VI 3	10	-	-	-	-	-	-
VI 4	10	-	-	-	-	-	-
VI 5	10	-	-	-	-	-	-
VI 6	10	-	-	-	-	-	-
VI 7	10	-	-	-	-	-	-
VI 8	10	-	-	-	-	-	-
VI 9	10	-	-	-	-	-	-
VI 10	10	-	-	-	-	-	-
VII 1	40	-	-	-	-	-	-
VII 2	40	-	-	-	-	-	-
VII 3	40	-	-	-	-	-	-
VII 4	40	-	-	-	-	-	-
VII 5	40	-	-	-	-	-	-
VII 6	40	-	-	-	-	-	-

6.6 Appendix C2: Specimen dimensions and SBS test results

Test#	Cyl.	Ring	Segm.	w [mm]	t [mm]	l [mm]	Peak load [N]	Apparent ILSS [MPa]
11	I	2	D	11.63	5.76	32.51	1188	13.30073087
12	I	2	E	11.66	5.72	31.04	1271	14.29263275
13	I	2	F	12.16	5.68	33.37	1235	13.41054137
14	I	2	G	11.81	5.56	35.43	1290	14.73419063
15	I	2	H	11.95	5.47	34.72	1357	15.56990201
16	I	4	D	11.99	4.64	32.91	1104	14.88309223
17	I	4	E	11.99	4.58	33.51	1190	16.25262683
18	I	4	F	11.96	4.6	35.58	1136	15.48640396
19	I	4	I	11.85	4.65	35.32	1133	15.42126038
20	I	4	H	11.8	4.59	36.46	1337	18.51390274
21	I	5	D	12.39	5.61	30.9	1144	12.34392062
22	I	5	E	12.63	5.61	33.38	1130	11.96116538

Test#	Cyl.	Ring	Segm.	w [mm]	t [mm]	l [mm]	Peak load [N]	Apparent ILSS [MPa]
23	I	5	F	12.15	5.61	34	1040	11.44341014
24	I	5	G	12.02	5.54	35.97	1119	12.60309232
25	I	5	H	12.17	5.63	34.09	1034	11.31834243
26	I	8	D	10.74	5.38	32.08	1154	14.97892048
27	I	8	E	11.79	5.4	32.42	1313	15.46743945
28	I	8	F	12.13	5.4	34.3	1642	18.80095264
29	I	8	G	11.59	5.37	34.64	1535	18.49745253
30	I	8	H	12.06	5.44	33.17	1426	16.30176324
31	I	9	D	11.71	5.49	30.96	2178	25.40913609
32	I	9	E	11.82	5.57	32.95	2226	25.35792726
33	I	9	F	12.11	5.6	33.06	2706	29.926566
34	I	9	G	12.32	6.51[4]	34.18	2554	23.88308696
35	I	9	H	12.01	5.45	34.87	2448	28.05001948
36	I	10	F	11.45	5.6	32.54	2234	26.13069245
37	I	10	G	11.64	5.6	33.37	2311	26.59011414
38	I	10	H	12.18	5.58	32.1	2715	29.96053816
39	I	10	I	11.79	5.64	34.55	2583	29.13350658
40	I	10	J	11.94	5.6	32.72	2399	26.90909907
1	IV	1	A	11.83	5.24	32.97	2431	29.41238151
2	IV	1	B	11.13	5.25	32.81	2520	32.34501348
3	IV	1	C	10.92	5.27	32.52	2306	30.05296411
4	IV	1	D	11.18	5.27	33.18	2128	27.08822002
5	IV	1	E	11.35	5.18	32.55	2443	31.16442434
70	IV	2	A	12.09	5.37	32.26	2836	32.76173577
71	IV	2	B	12.15	5.43	33.14	2984	33.92219721
72	IV	2	C	12.21	5.41	33.12	2895	32.86978795
73	IV	2	D	12.32	5.33	33.36	2924	33.39648157
74	IV	2	E	12.03	5.37	32.89	2884	33.482402
75	IV	3	A	12.46	5.39	32.4	2927	32.68715921
76	IV	3	B	11.31	5.46	32.52	2606	31.65048921
77	IV	3	C	12.03	5.32	33.98	2936	34.40646504
78	IV	3	D	12.33	5.4	33.98	2857	32.18212129
79	IV	3	E	12.25	5.42	32.94	2884	32.57775435
81	IV	4	A	12.19	5.34	32.76	2891	33.30921459
82	IV	4	B	12.21	5.41	32.29	2781	31.57543361
83	IV	4	C	12.22	5.43	32.37	2855	32.26980496
84	IV	4	D	11.97	5.37	33.12	2693	31.42166403
85	IV	4	E	12.32	5.33	32.76	2739	31.28350308
86	IV	5	A	12.33	5.29	33.14	2988	34.35762284
87	IV	5	B	12.23	5.37	33.81	2945	33.63146763
88	IV	5	C	12.28	5.33	33.72	3043	34.86885126
89	IV	5	D	12.3	5.25	31.66	2784	32.33449477

[4] Abnormally thick

Test#	Cyl.	Ring	Segm.	w [mm]	t [mm]	l [mm]	Peak load [N]	Apparent ILSS [MPa]
90	IV	5	E	12.19	5.26	32.91	2924	34.20181723
91	IV	6	A	12.23	5.17	32.21	3013	35.73908216
92	IV	6	B	12.23	5.22	33.38	2976	34.96207742
93	IV	6	C	12.16	5.16	33.64	2891	34.55620793
94	IV	6	D	12.14	5.17	31.83	2909	34.76127959
95	IV	6	E	11.82	5.22	32.82	2994	36.39360523
96	IV	7	A	12.06	5.3	33.33	2926	34.33305172
97	IV	7	B	12.22	5.28	33.8	2931	34.06998587
98	IV	7	C	12.23	5.24	33.21	2847	33.31892543
99	IV	7	D	12.09	5.14	33.3	3005	36.26739145
100	IV	7	E	12.22	5.14	34.04	3098	36.99204595
41	II	1	A	11.83	5.23	32.74	1514	18.35273125
42	II	1	B	11.67	5.16	32.65	1324	16.4903051
43	II	1	C	12.06	5.12	32.41	1155	14.02897621
44	II	1	D	11.45	5.26	33.46	1567	19.51367327
45	II	1	E	11.62	5.25	32.21	1470	18.07228916
46	II	2	A	12.24	5.41	32.2	1498	16.96658331
47	II	2	B	12.24	5.35	33.3	1479	16.93925234
80	II	2	C	11.94	5.43	32.77	1322	15.2928547
48	II	2	D	11.43	5.41	32.8	1254	15.20951286
49	II	2	E	11.97	5.56	32.27	1399	15.76558302
50	II	3	A	11.73	5.66	32.8	1685	19.03473019
51	II	3	B	11.63	5.59	30.79	1518	17.51223241
52	II	3	C	12.21	5.61	32.56	1650	18.06619454
53	II	3	D	12.55	5.79	32.66	1747	18.03150094
54	II	3	E	12.23	5.81	32.15	1646	17.37354745
55	II	4	A	11.96	5.56	33.12	953	10.74850822
56	II	4	B	11.99	5.52	32.28	1024	11.60387279
57	II	4	C	11.99	5.52	33.37	894	10.13072488
58	II	4	D	12.34	5.7	33.15	923	9.841764054
59	II	4	E	12.38	5.65	32.54	1171	12.55593521
60	II	5	A	12.05	5.73	33.18	1220	13.25193891
61	II	5	B	12.01	5.7	32.13	1134	12.42385731
62	II	5	C	12.11	5.72	33.24	1151	12.46224873
63	II	5	D	12.02	5.72	32.71	1320	14.39907846
64	II	5	E	12.04	5.75	33.77	1210	13.10847898
65	II	6	A	12.21	5.51	33.79	1415	15.77431251
66	II	6	B	12.09	5.56	32.13	1445	16.12233786
67	II	6	C	11.93	5.56	32.99	1303	14.73297473
68	II	6	D	11.82	5.6	33.08	1278	14.48060189
69	II	6	E	12.1	5.61	32.52	1333	14.72797985
101	V	1	A	12.1	5.09	32.83	1726	21.01836367
102	V	1	B	12.28	5.05	33.35	1601	19.36256329
103	V	1	C	12.41	5.07	34.14	1842	21.95690629

Test#	Cyl.	Ring	Segm.	w [mm]	t [mm]	l [mm]	Peak load [N]	Apparent ILSS [MPa]
104	V	1	D	12.26	5.06	33.77	1923	23.24874749
105	V	1	E	12.03	5.05	32.92	1779	21.96242068
106	V	2	A	12.39	5.06	32.36	2075	24.82318713
107	V	2	B	12.47	5.05	32.89	1976	23.53370862
108	V	2	C	12.34	5.05	33.82	2133	25.67116517
109	V	2	D	12.32	5.04	33.1	1959	23.66216373
110	V	2	E	12.17	5.02	33.55	2231	27.3883922
111	V	3	A	12.19	5.17	33.95	2351	27.97819185
112	V	3	B	12.05	5.18	32.36	2540	30.51955334
113	V	3	C	12.07	5.15	33.69	2608	31.46692835
114	V	3	D	12.08	5.15	33.54	2456	29.60843567
115	V	3	E	11.86	5.16	32.39	2478	30.36883799
116	V	4	A	12.27	5.17	33.19	2359	27.89035861
117	V	4	B	12.21	5.08	33.16	2922	35.33150187
118	V	4	C	12.31	5.19	33.3	2780	32.63477693
119	V	4	D	12.24	5.12	33.05	2717	32.5161803
120	V	4	E	12.1	5.14	33.58	2636	31.78763225
121	V	5	A	12.15	5.22[5]	33.45	2347	27.75412705
122	V	5	B	11.84	5.01	32.27	2495	31.54586098
123	V	5	C	12.15	5.02	32.63	2118	26.04397226
124	V	5	D	12.14	5.06	33.46	2486	30.35241029
125	V	5	E	12.09	5.01	32.72	2503	30.99260536
126	V	6	A	12.3	5.09	32.18	1869	22.38966889
127	V	6	B	12.36	5.09	32.58	1969	23.473115
128	V	6	C	12.36	4.95	33.03	1904	23.3401981
129	V	6	D	12.16	5.04	32.28	2034	24.89132989
130	V	6	E	12.26	4.96	33.43	1945	23.98881098
131	V	7	A	12.11	5.1	31.82	2181	26.48516054
132	V	7	B	12.06	4.99	33.11	1926	24.00323034
133	V	7	C	12	5	33.59	2059	25.7375
134	V	7	D	12.13	4.91	31.63	2030	25.56318767
135	V	7	E	12.17	4.89	33.16	2085	26.27652227
136	V	8	A	12.12	5.1	32.96	-	-
137	V	8	B	12.29	5.38	33.26	-	-
138	V	8	C	12.34	5.38	33.2	-	-
139	V	8	D	12.25	5.33	32.57	-	-
140	V	8	E	12.22	5.33	32.45	-	-
141	V	9	A	-	-	-	-	-
142	V	9	B	-	-	-	-	-
143	V	9	C	-	-	-	-	-
144	V	9	D	-	-	-	-	-

[5] Anomalous bump in thickness, could be something caught in between the composite, such as carbon fibre fluff

Test#	Cyl.	Ring	Segm.	w [mm]	t [mm]	l [mm]	Peak load [N]	Apparent ILSS [MPa]
145	V	9	E	-	-	-	-	-
146	V	10	A	-	-	-	-	-
147	V	10	B	-	-	-	-	-
148	V	10	C	-	-	-	-	-
149	V	10	D	-	-	-	-	-
150	V	10	E	-	-	-	-	-
6	VI	1	A	11.42	5.18	34.06	2659	33.71193936
7	VI	1	B	11.46	5.14	34.55	2734	34.81064233
8	VI	1	C	11.39	5.18	33.58	2721	34.5888658
9	VI	1	D	11.42	5.11	34.39	2811	36.12726668
10	VI	1	E	11.13	5.19	33.42	2472	32.09572628
151	VI	2	A	-	-	-	-	-
152	VI	2	B	-	-	-	-	-
153	VI	2	C	-	-	-	-	-
154	VI	2	D	-	-	-	-	-
155	VI	2	E	-	-	-	-	-
156	VI	3	A	-	-	-	-	-
157	VI	3	B	-	-	-	-	-
158	VI	3	C	-	-	-	-	-
159	VI	3	D	-	-	-	-	-
160	VI	3	E	-	-	-	-	-
161	VI	4	A	-	-	-	-	-
162	VI	4	B	-	-	-	-	-
163	VI	4	C	-	-	-	-	-
164	VI	4	D	-	-	-	-	-
165	VI	4	E	-	-	-	-	-
166	VI	5	A	-	-	-	-	-
167	VI	5	B	-	-	-	-	-
168	VI	5	C	-	-	-	-	-
169	VI	5	D	-	-	-	-	-
170	VI	5	E	-	-	-	-	-
171	VI	6	A	-	-	-	-	-
172	VI	6	B	-	-	-	-	-
173	VI	6	C	-	-	-	-	-
174	VI	6	D	-	-	-	-	-
175	VI	6	E	-	-	-	-	-
176	VI	7	A	-	-	-	-	-
177	VI	7	B	-	-	-	-	-
178	VI	7	C	-	-	-	-	-
179	VI	7	D	-	-	-	-	-
180	VI	7	E	-	-	-	-	-
181	VI	8	A	-	-	-	-	-
182	VI	8	B	-	-	-	-	-
183	VI	8	C	-	-	-	-	-

Test#	Cyl.	Ring	Segm.	w [mm]	t [mm]	l [mm]	Peak load [N]	Apparent ILSS [MPa]
184	VI	8	D	-	-	-	-	-
185	VI	8	E	-	-	-	-	-
186	III	1	A	-	-	-	-	-
187	III	1	B	-	-	-	-	-
188	III	1	C	-	-	-	-	-
189	III	1	D	-	-	-	-	-
190	III	1	E	-	-	-	-	-
191	III	1	F	-	-	-	-	-
192	III	1	G	-	-	-	-	-

6.7 Appendix D: SBS load-displacement curves

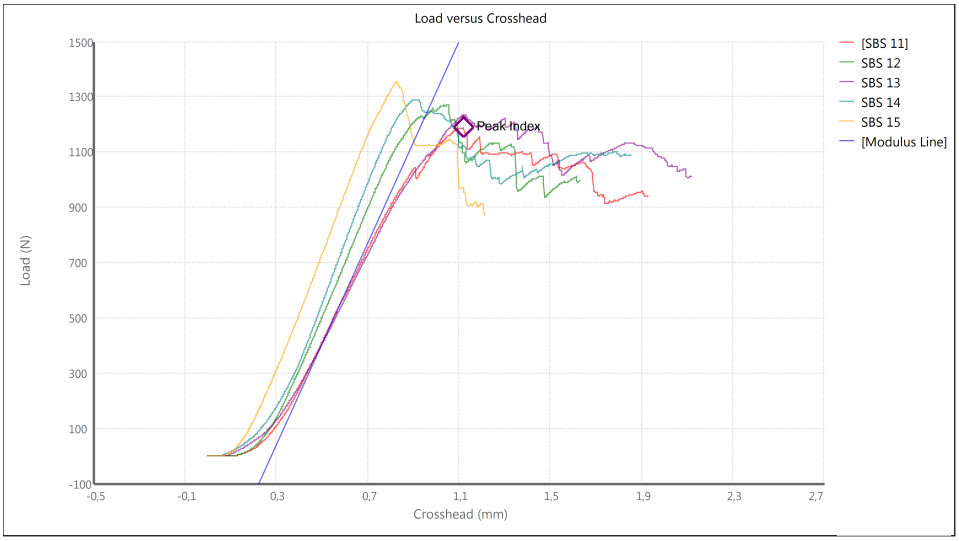

Figure 6.4: Load-displacement curve for SBS of ring I2

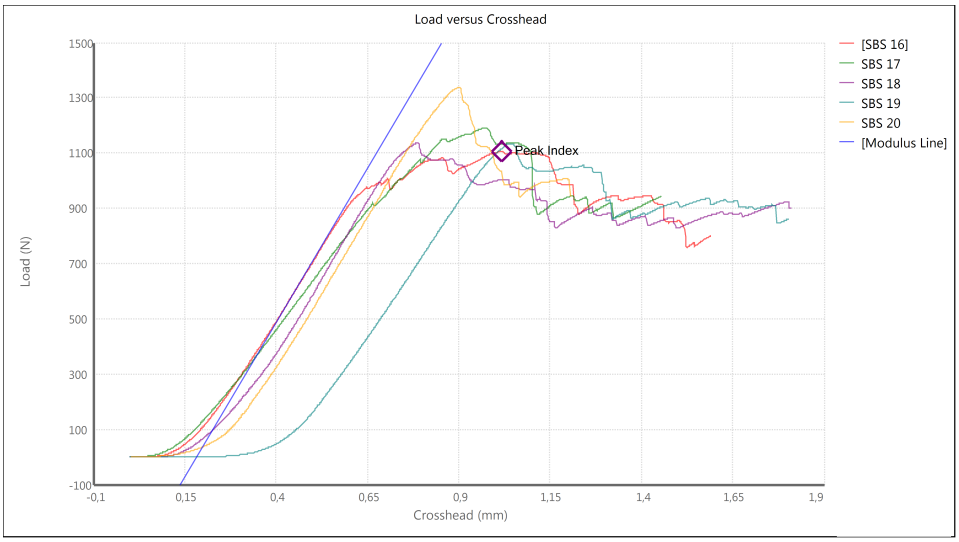

Figure 6.5: Load-displacement curve for SBS of ring I4

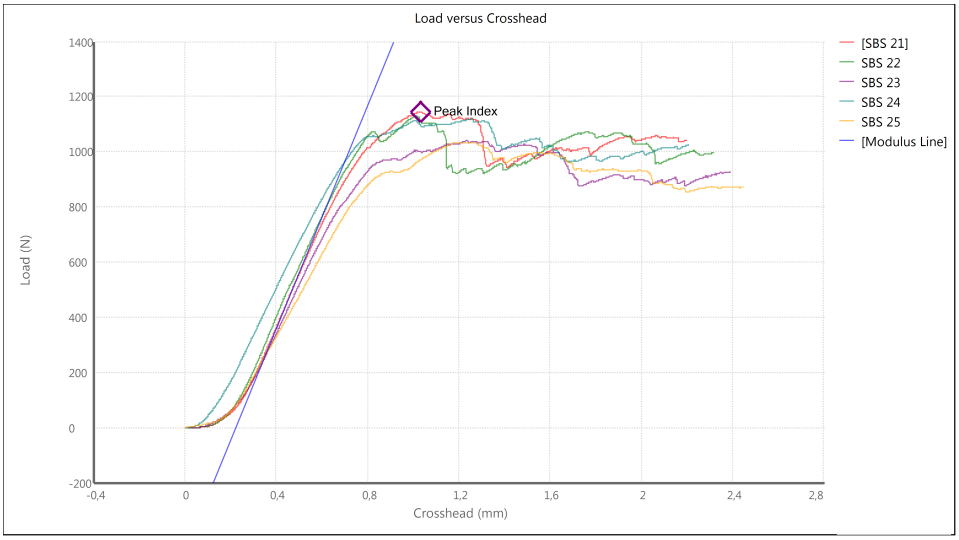

Figure 6.6: Load-displacement curve for SBS of ring I5

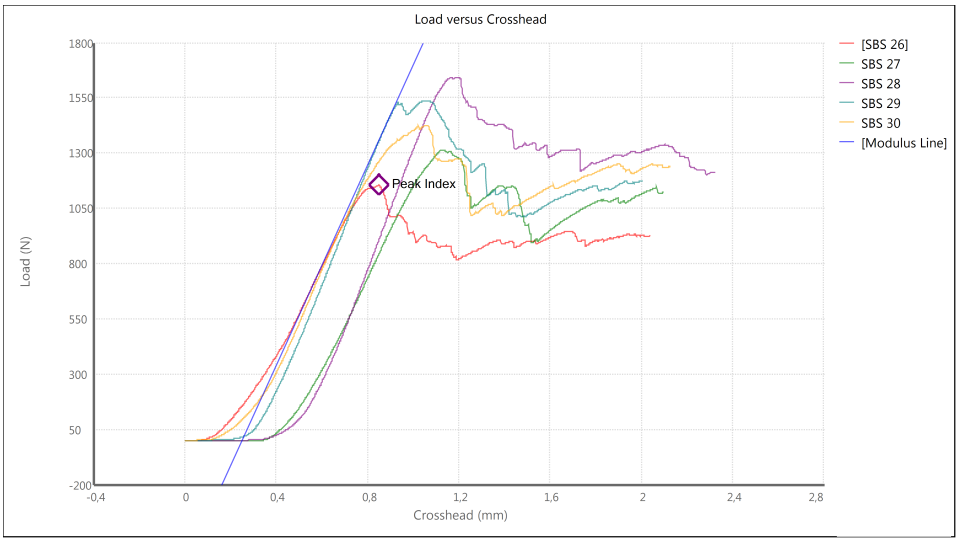

Figure 6.7: Load-displacement curve for SBS of ring I8

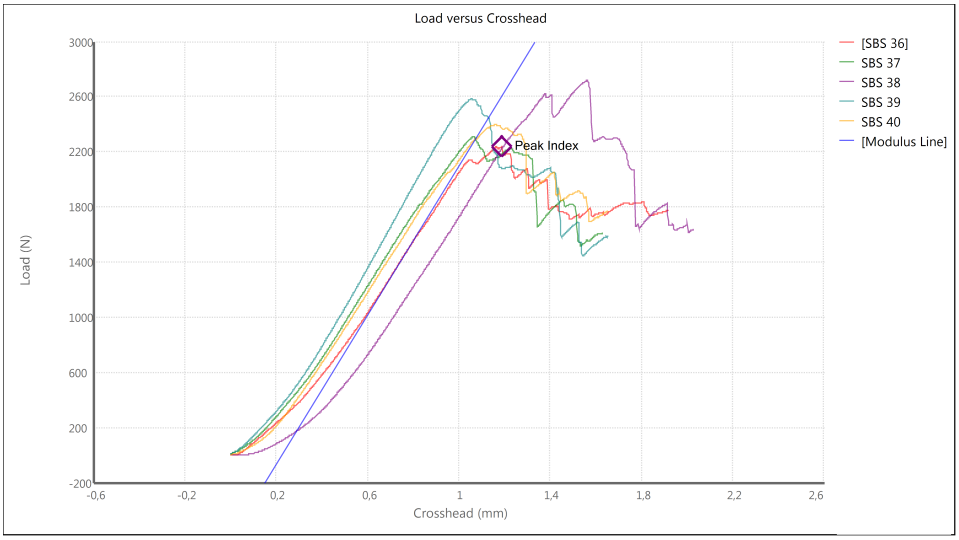

Figure 6.8: Load-displacement curve for SBS of ring I10

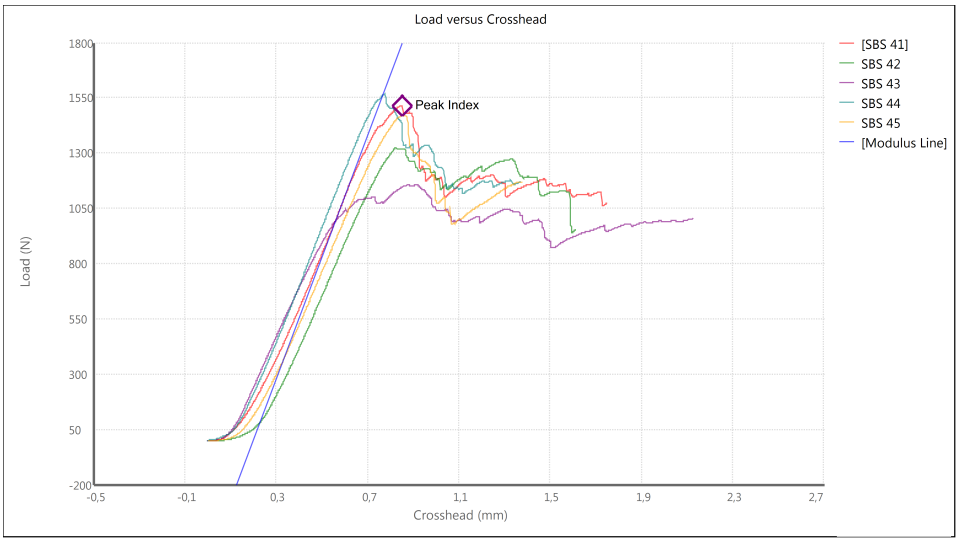

Figure 6.9: Load-displacement curve for SBS of ring II1

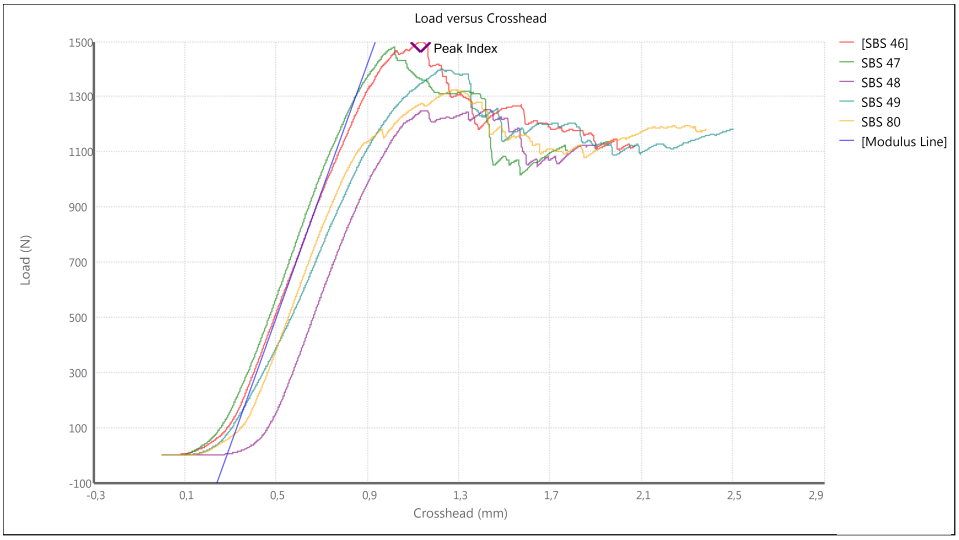

Figure 6.10: Load-displacement curve for SBS of ring II2

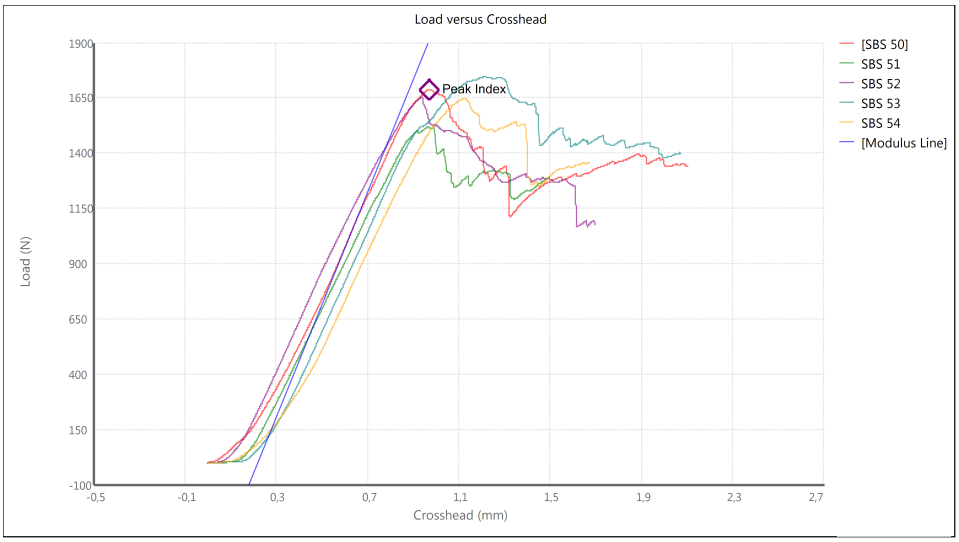

Figure 6.11: Load-displacement curve for SBS of ring II3

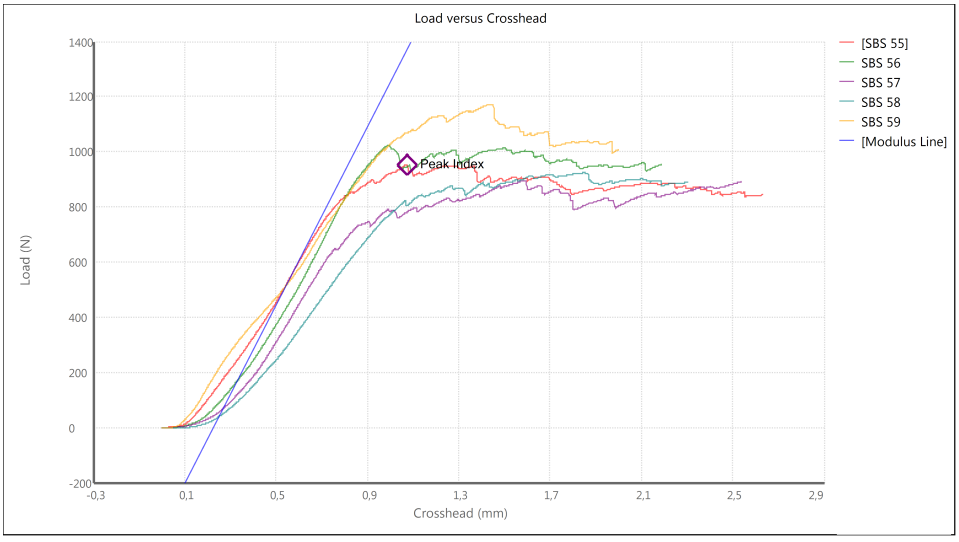

Figure 6.12: Load-displacement curve for SBS of ring II4

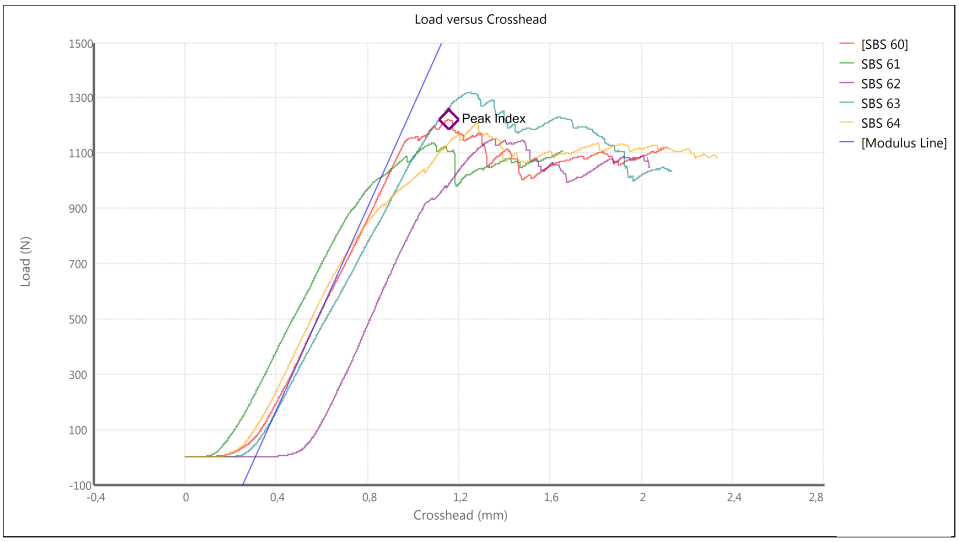

Figure 6.13: Load-displacement curve for SBS of ring II5

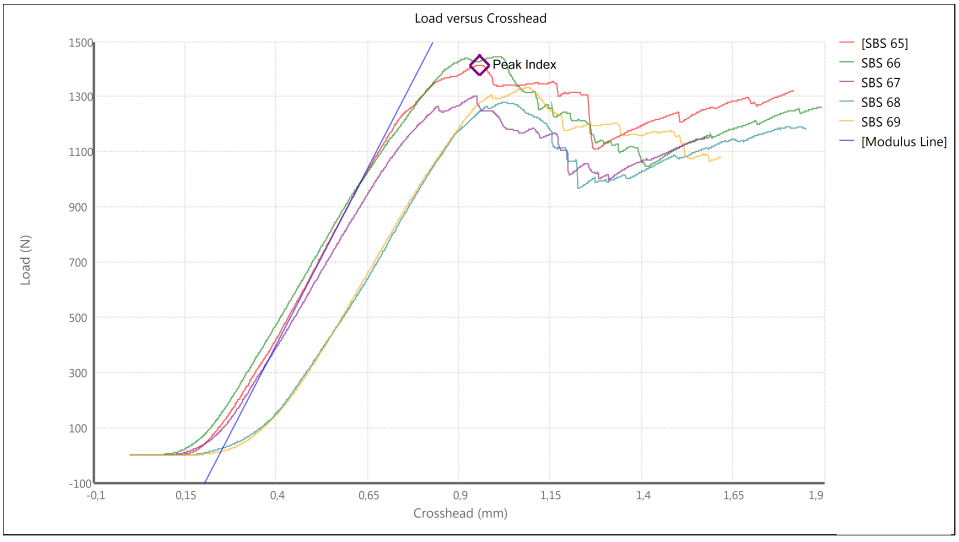

Figure 6.14: Load-displacement curve for SBS of ring II6

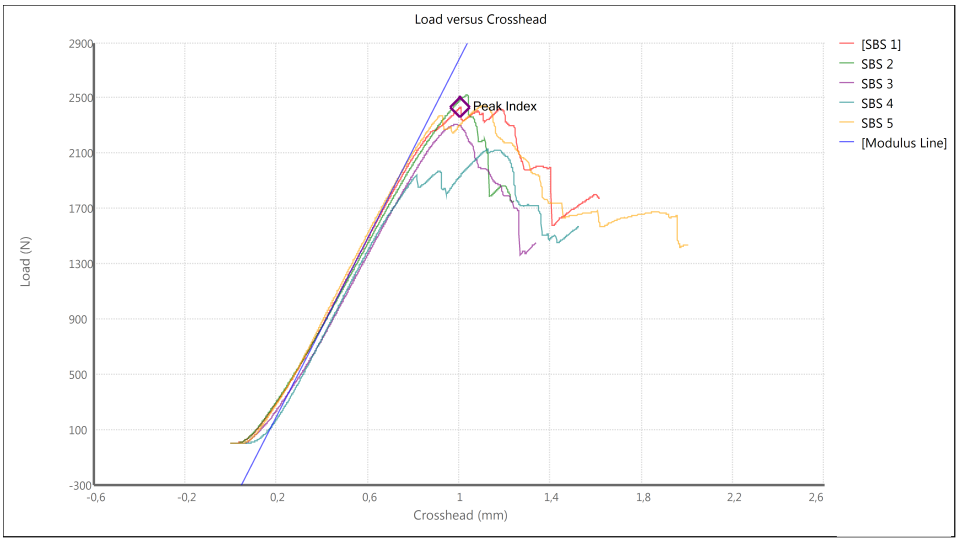

Figure 6.15: Load-displacement curve for SBS of ring IV1

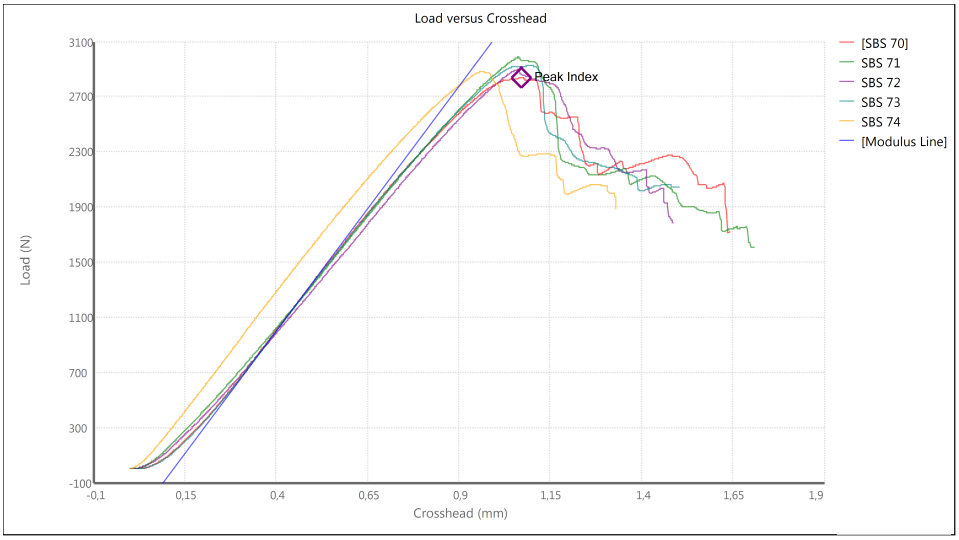

Figure 6.16: Load-displacement curve for SBS of ring IV2

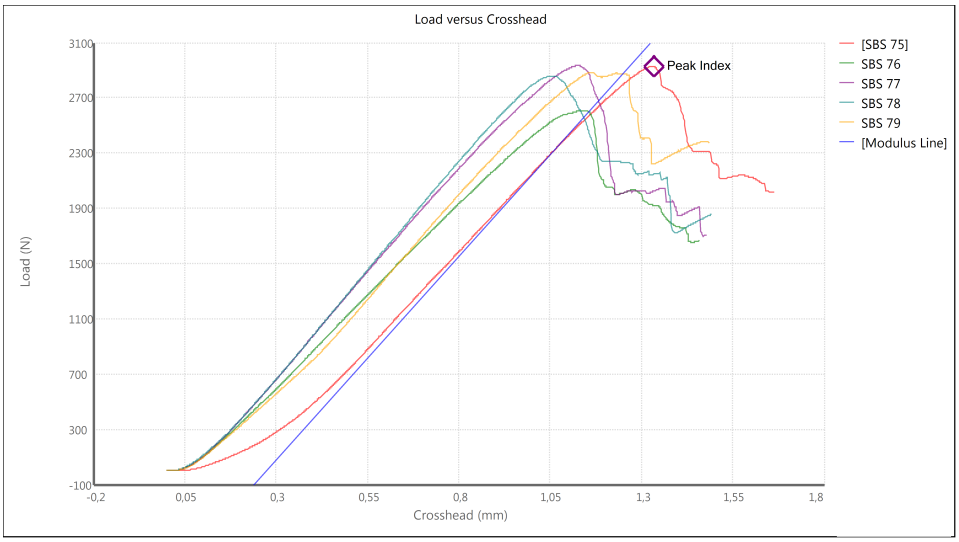

Figure 6.17: Load-displacement curve for SBS of ring IV3

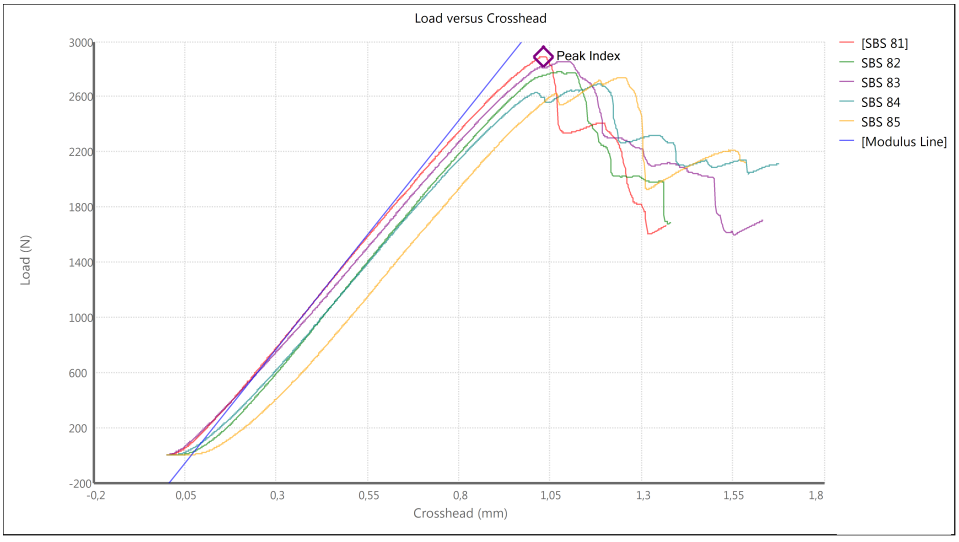

Figure 6.18: Load-displacement curve for SBS of ring IV4

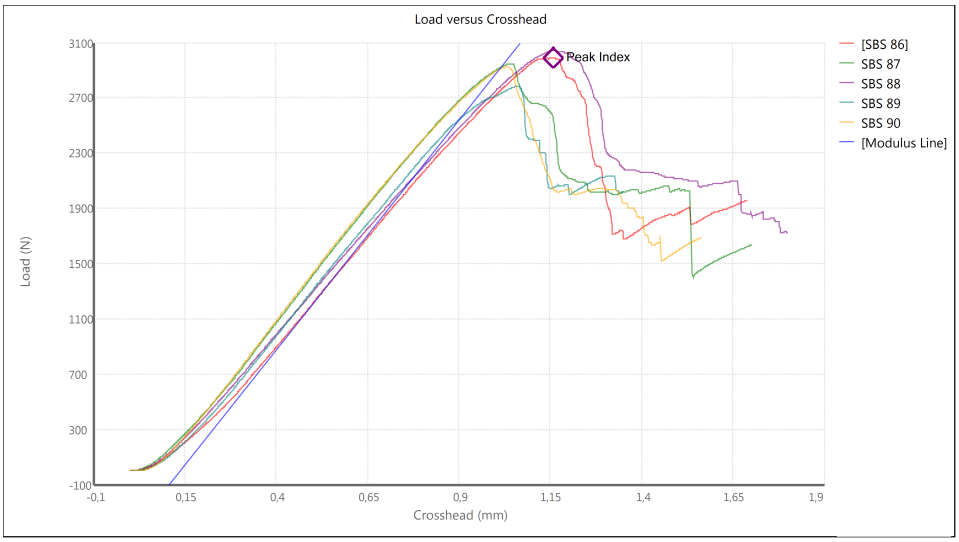

Figure 6.19: Load-displacement curve for SBS of ring IV5

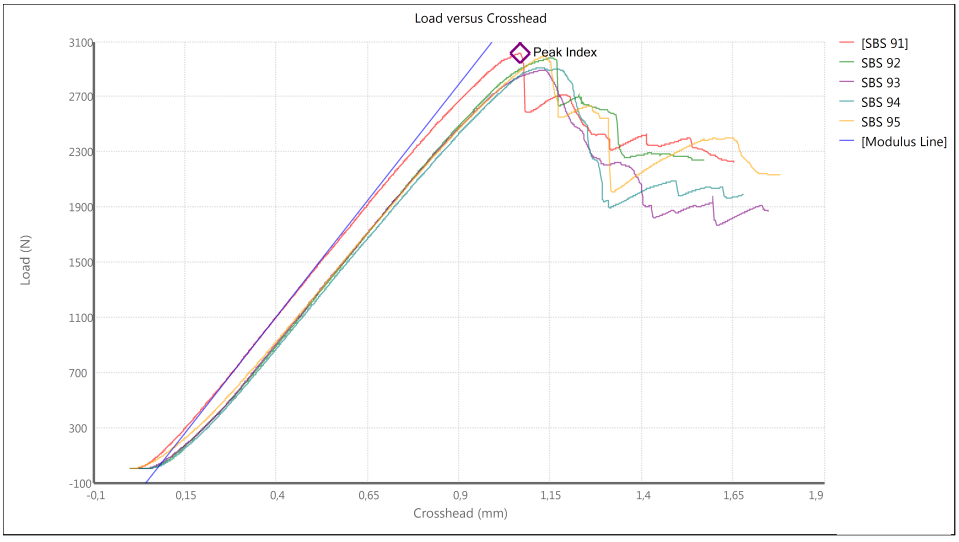

Figure 6.20: Load-displacement curve for SBS of ring IV6

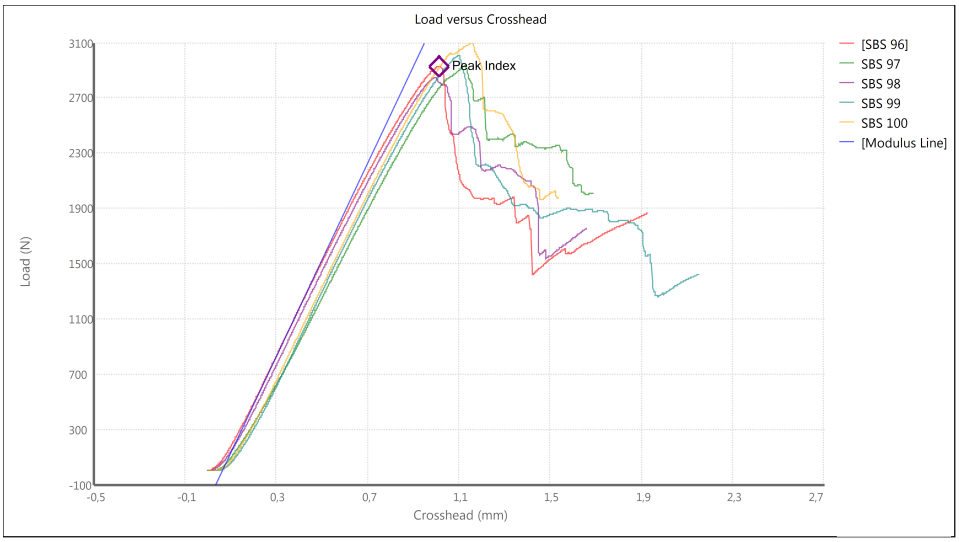

Figure 6.21: Load-displacement curve for SBS of ring IV7

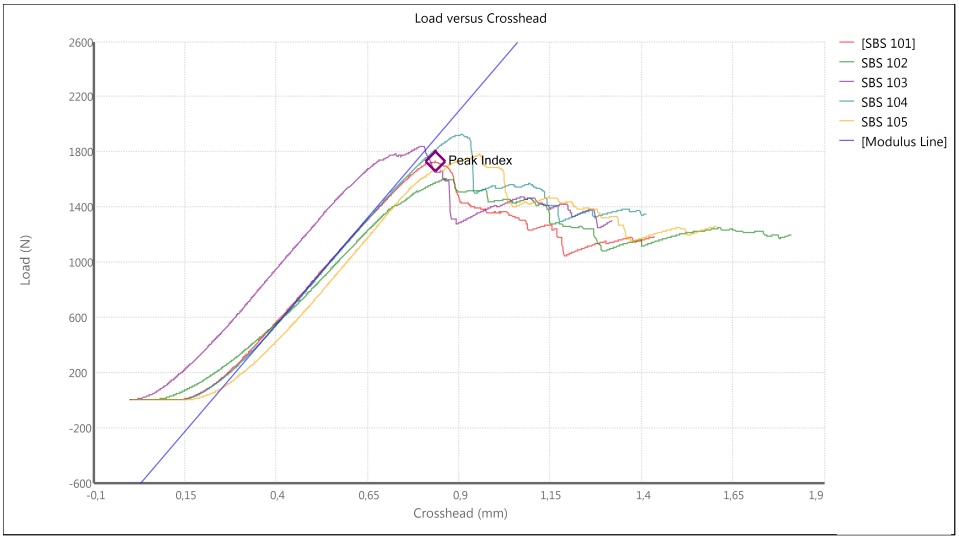

Figure 6.22: Load-displacement curve for SBS of ring V1

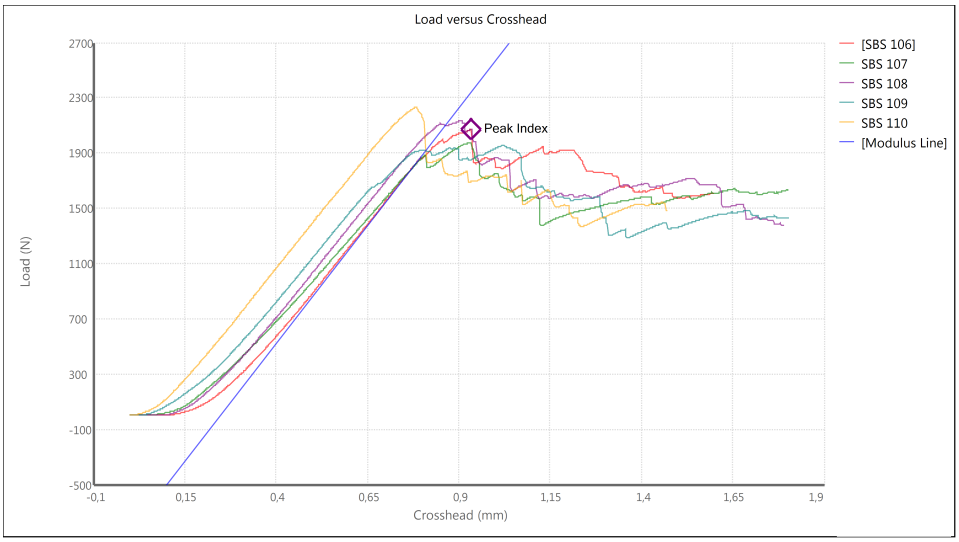

Figure 6.23: Load-displacement curve for SBS of ring V2

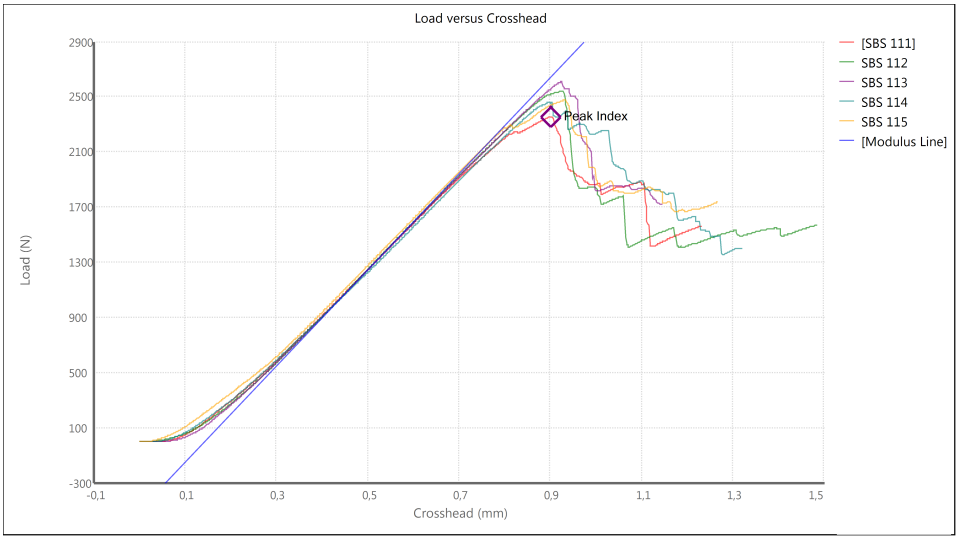

Figure 6.24: Load-displacement curve for SBS of ring V3

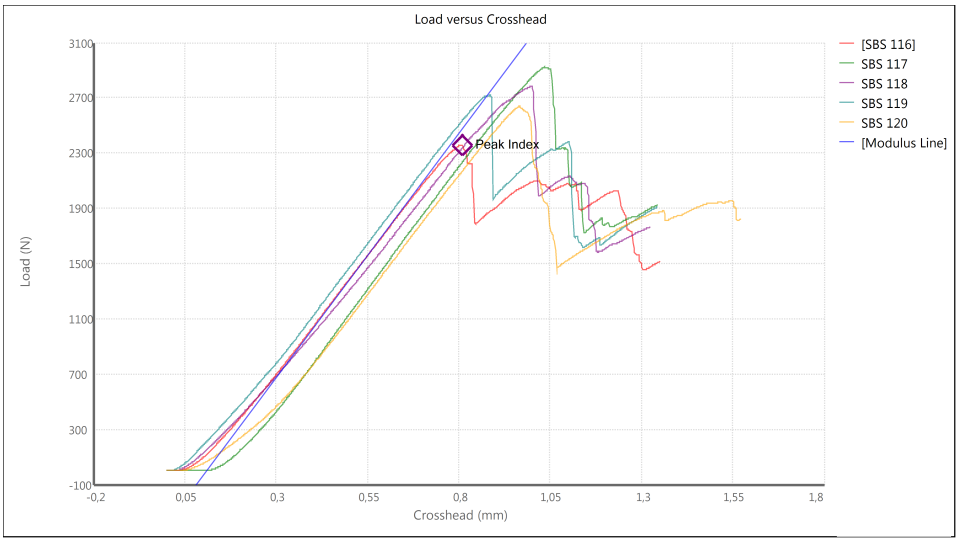

Figure 6.25: Load-displacement curve for SBS of ring V4

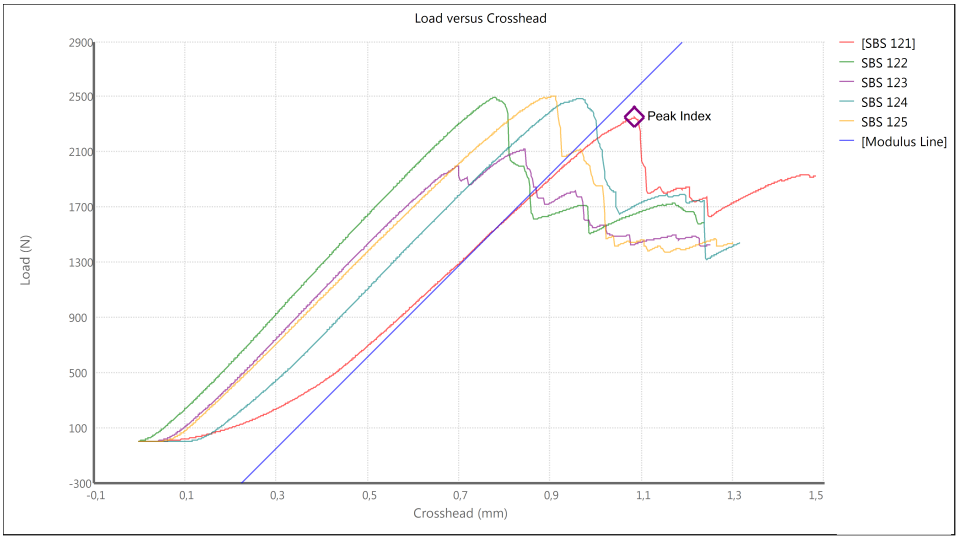

Figure 6.26: Load-displacement curve for SBS of ring V5

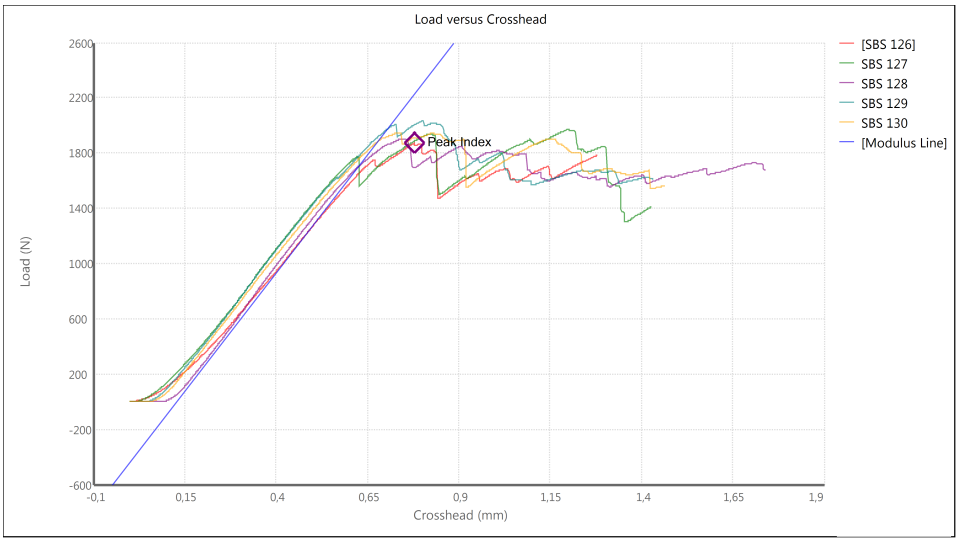

Figure 6.27: Load-displacement curve for SBS of ring V6

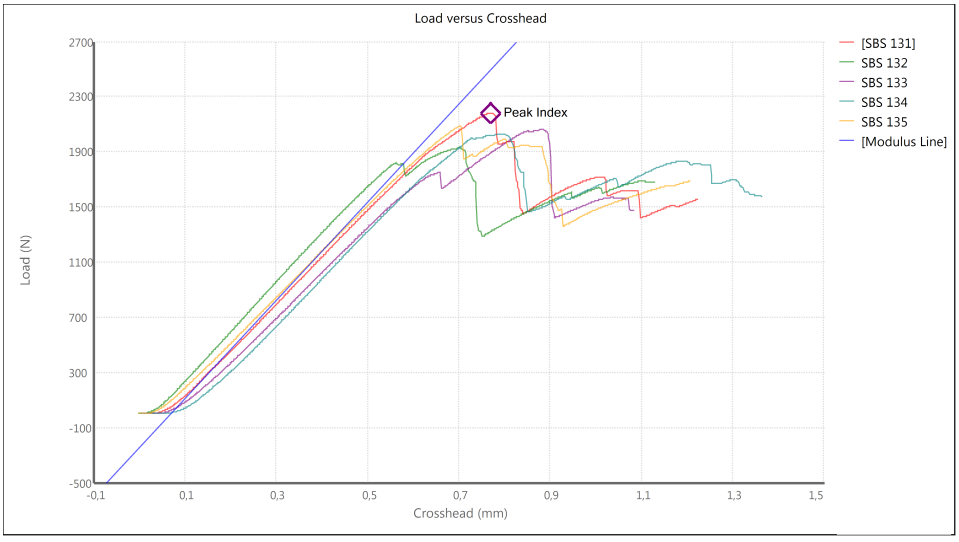

Figure 6.28: Load-displacement curve for SBS of ring V7

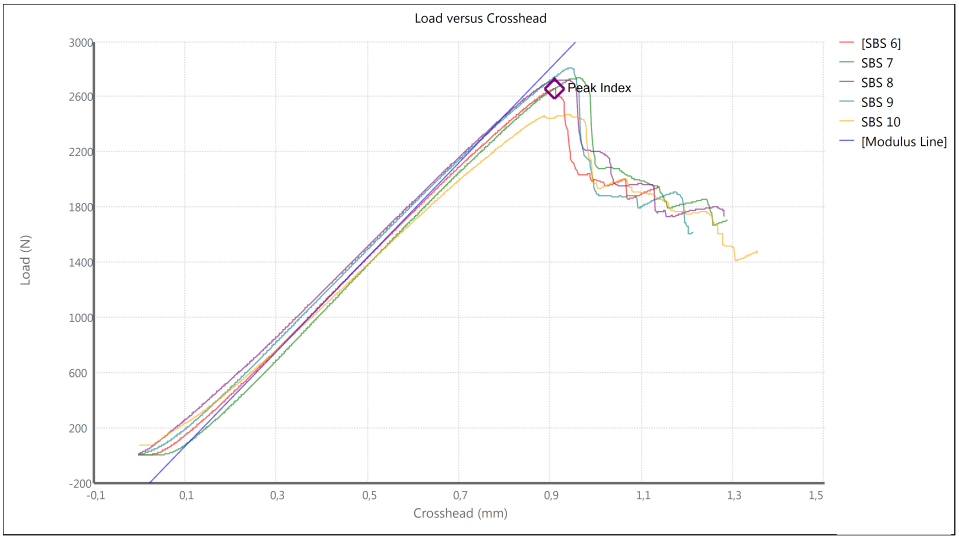

Figure 6.29: Load-displacement curve for SBS of ring VI1

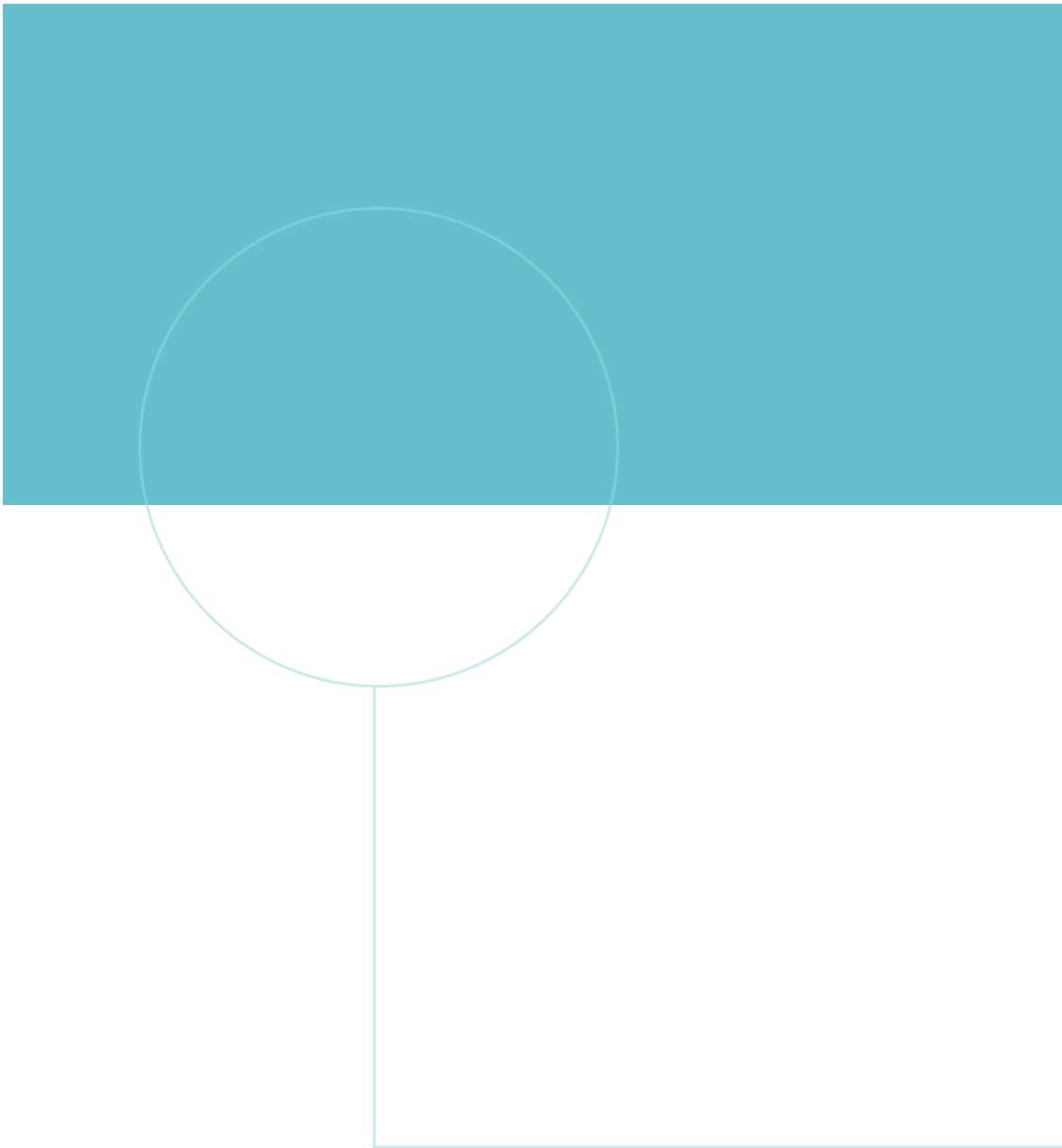

NTNU
Norwegian University of
Science and Technology

HEXAGON